THESIS TITLE

MODELING AND SIMULATION OF CARBON DIOXIDE ABSORPTION INTO PROMOTED MDEA SOLUTION AT INDUSTRIAL PACKED COLUMN

DUAA ABDELMONEM AMIN ALI
NRP 2314201702

Supervisors:
Prof. Dr. Ir. Ali Altway, MS.
NIP. 1951 08 04 1974 12 1001

Dr.Ir. Susiantu DEA
NIP.1962 08 20 1989 03 1004

MASTER PROGRAM

CHEMICAL ENGINEERING DEPARTMENT

FACULTY OF INDUSTRIAL TECHNOLOGY

SEPULUH NOPEMBER INSTITUTE OF TECHNOLOGY

SURABAYA 2016

APROVAL SHEET

MODELING AND SIMULATION OF CARBON DIOXIDE ABSORPTION INTO PROMOTED MDEA SOLUTION AT INDUSTRIAL PACKED COLUMN

The thesis is structured to comply with one of the requirements to holds a
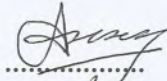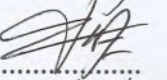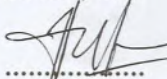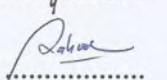Master of Engineering (MT)

in

Institut Teknologi Sepuluh November Surabaya

By:

Duaa Abdelmonem Amin Ali
NRP. 23 14 201 702
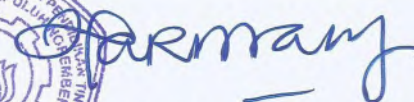
Date of Exam	: 14 July 2016
Graduation period	: September 2016

Approved by :

1. Prof. Dr. Ir. Ali Altway , MSc.   (Supervisor)
    NIP. 1951 08 04 1974 12 1001

2. Dr. Ir.Susianto , DEA.   (Co. Supervisor)
    NIP. 1951 08 04 1974 12 1001

3. Prof. Dr. Ir. Gede Wibawa , M.Eng   (Examiner)
    NIP. 1963 01 22 1987 01 1001

4. Dr. Yeni Rahmawati , S.T. , M.T   (Examiner)
    NIP. 1976 10 20 2005 01 2001

Director of Graduate Programs,

Prof. Ir. Djauhar Manfaat , M.Sc , Ph.D
NIP. 1960 12 02 1987 01 1001

MODELING AND SIMULATION OF CARBON DIOXIDE ABSORPTION INTO PROMOTED MDEA SOLUTION AT INDUSTRIAL PACKED COLUMN

Student Name   : Duaa Abdelmonem Amin Ali

Advisors   : 1. Prof. Dr. Ir. Ali Altway, MS.

                     2. Dr.Ir. Susiantu DEA

ABSTRACT

The global warming caused by increasing emission of carbon dioxide is one of the most serious environmental problems. Following the 1997 Kyoto Protocol, the European Union has set a goal of 20% reduction of CO_2 emission by the year 2020. In order to meet this target, a significant reduction of CO_2 release from fossil fuel fired thermal power plants, will be required. Therefore, removal of carbon dioxide from flue gases is a key measure to reduce CO_2 emission. Chemical absorption is the most practical and effective technique and is widely used in chemical and petrochemical industry and well suited for CO_2 capture for industrial applications. A suitable solvent for CO_2 absorption must be properly selected in the capture process, since the solvent affects equipment sizing and operating costs. MDEA as a solvent has been favored in the past few years because of its many advantages over other amines. However, the main disadvantage of this solvent is its slow reaction rate with CO_2 for this reason; an activator with a very high reaction rate with CO_2 must be added. Potassium glycinate which has distinguishing feature of fast reaction kinetics present a suitable promoter and can act as an enhancer for MDEA when reacting with CO_2.

Process simulation is an essential tool for the study of chemical processes because of its ability to predict process performance with adjustments in key parameters, hence bypassing expensive and time-consuming testing or experiments in pilot plants. Many researchers have simulated the CO_2 absorption from power plants and chemical processes through literature.

Following the work of previous researchers, in this research a mathematical model of reactive absorption of CO_2 into promoted MDEA with piperazine at packed column has been created. Validation of the created mathematical model has been done on actual data of absorber in an existing natural gas sweetening process in Thailand called Acid Gas Removal Unit (AGRU).which is also using a solvent MDEA and piperazine as a promoter the obtained error is 3.723%.

The second part of this study is developing a simulation model with an amino acid promoter, potassium glycinate, instead of piperazine in the same gas feed condition and column configurations. the influence of various operating variables such as potassium glycinate concentration, solvent feed flow rate, feed temperature of both gas and liquid stream, and finally the pressure of the absorber on CO_2 absorptive capability have been examined theoretically.

Keyword: Absorption, Chemical Absorption, Carbon dioxide, MDEA, Packed column, Mathematical model, piperazine, potassium glycinate.

TABLE OF CONTENT

[This page is deliberately left blank]

LIST OF TABLES

[This page is deliberately left blank]

LIST OF FIGURES

[This page is deliberately left blank]

Notation

a_i	Constant in The temperature dependence of the equilibrium constants expression	
a	Gas-liquid interfacial area per unit volume of packed column	$[m^2 . m^{-3}]$
a_p	Specific area of packing	$[m^2 . m^{-3}]$
A	Sectional area of the column	$[m^2]$
$[A]$	Concentration of species A	$[kmole . m^{-3}]$
$[A]_e$	Equilibrium concentration of species A	$[kmole . m^{-3}]$
$[Am]_B$	Concentration of amine in the bulk solution	$[kmole . m^{-3}]$
b_i	Constant in The temperature dependence of the equilibrium constants expression	
c_i	Constant in The temperature dependence of the equilibrium constants expression	
c_{iL}	concentration of ion i	$[kmole . m^{-3}]$
C_{pG}	Gas heat capacity	$[J . kg^{-1} . K^{-1}]$
C	Molar density	$[kmole . m^{-3}]$
$[D]$	Matrix of Fick diffusion coefficients	$[m^2 . s^{-1}]$
$D_{A,L}$	diffusion coefficient of component A in the liquid phase	$[m^2 . s^{-1}]$
di	Driving force for mass diffusion	$[m^{-1}]$
D_{ij}	Infinite dilution diffusivity for component / present in trace amounts in component j	$[m^2 . s^{-1}]$
D_{MDEA}	Diffusion coefficient of MDEA in water	$[m^2 . s^{-1}]$
$D_{CO2,L}$	Diffusion coefficient of CO2 in the liquid phase	$[m^2 . s^{-1}]$
d_p	Nominal packing size	$[m]$
E	Enhancement factor	$[-]$
F_{rL}	Froude number	$[-]$
$[Glyk]_0$	Initial potassium glycinate concentration in the solution	$[kmole . m^{-3}]$
G	Mass velocity of gas	$[kg . m^{-2} . s^{-1}]$
$H_{e,jw}$	Henry constant of gas-water system	$[Pa . m^3 . kmole^{-1}]$
$\overline{h_G}$	Gas side heat transfer coefficient	$[W . m^{-2} . K^{-1}]$
hi	Ion-specific parameter	$[m^3 . kmole^{-1}]$
h_G	Gas specific parameter	$[m^3 . kmole^{-1}]$

h_T	Temperature correction	$[m^3 . kmole^{-1}]$
J	Mass diffusion flux relative to the mass average velocity	$[kg . m^{-2} . s^{-1}]$
k	Kinetic constant of the chemical reaction between absorbed component A and solvent component B	$[m^3 . kmole^{-1} . s^{-1}]$
k_b	Rate constant of the base protonation	$[m^3 . kmole^{-1} . s^{-1}]$
k_f	Forward reaction rate constant of equation (2.41)	$[m^3 . kmole^{-1} . s^{-1}]$
K_{eq}	Equilibrium constant	
k_{H2O}	Rate constant of reaction (2.50)	$[s^{-1}]$
k_L	Liquid side Mass transfer coefficient	$[m . s^{-1}]$
$\bar{k}_{L.av}$	The average mass transfer coefficient during a time interval tc	$[m . s^{-1}]$
k_{obs}	Observed reaction rate constant	$[s^{-1}]$
k_{OH^-}	Rate constant of reaction (2.50)	$[s^{-1}]$
k_{ov}	Overall pseudo first order rate constant	$[s^{-1}]$
k_r	Reverse reaction rate constant of equation (2.41)	$[m^3 . kmole^{-1} . s^{-1}]$
$\acute{k}$	Forward reaction rate constant of equation (2.49)	$[m^3 . kmole^{-1} . s^{-1}]$
k_2	Second order rate constant	$[m^3 . kmole^{-1} . s^{-1}]$
K_1	Equilibrium constant of reaction (2.56)	$[m^3 . kmole^{-1}]$
K_2	Equilibrium constants of reaction (2.57)	$[m^3 . kmole^{-1}]$
K_3	Equilibrium constants of reaction (2.58)	[-]
K_4	Equilibrium constants of reaction (2.59)	[-]
K_5	Equilibrium constants of reaction (2.60)	[-]
k_L^o	Liquid side Physical mass transfer coefficient	$[m . s^{-1}]$
k_G	Gas side mass transfer coefficient	$[kmole . m^{-2} atm^{-1} s^{-1}]$
ℓ	Generalized characteristic length	$[m]$
L	Mass velocity of liquid	$[kmole . m^{-2} s^{-1}]$
L_{in}	Inlet molar flow rate of liquid	$[kmole . s^{-1}]$
M	Hatta Number	[-]
$[MDEA]_B$	Bulk concentration of MDEA in the solution	$[kmole . m^{-3}]$

Mi	Molecular weight of component i	[kg. kmole^{-1}]
N_i	Molar flux of component / referred to a stationary coordinate reference frame	[kmole.m^{-2}.s^{-1}]
N_t	Mixture molar flux referred to a stationary coordinate reference frame	[kmole.m^{-2}. s^{-1}]
N_{CO2}	Molar flux (absorption flux) of CO2	[kmole.m^{-2}.s^{-1}]
P_{rG}	Prandtl number for the gas side	[-]
r	Coordinate direction or position	[m]
r_δ	Outer edge of film	[m]
R	Gas constant in	[$joule. kmole^{-1}. K^{-1}$]
R_A	Rate of reaction of A	[kmole.m^{-3}. s^{-1}]
r_{ovrall}	Overall reaction rate	[kmole. m^{-3} .s^{-1}]
R_{eG}	Reynold number of gas	[-]
R_{eL}	Reynold number of liquid	[-]
R_{CO_2}	Reaction rate of CO2	[kmol. m^{-3} .s^{-1}]
S_{cG}	Schmidt number of gas	[-]
S_{cL}	Schmidt number of liquid	[-]
s	Surface renewal frequency	[s^{-1}]
t	Time	[s]
T	Temperature	[K]
u_i	Velocity of diffusion of species i	[m. s^{-1}]
v_i	Molar flow rate of component i	[kmole. s^{-1}]
x_i	Mole fraction of component i in liquid phase	[-]
X	Distance from the interface	[m]
X_i	Molar ratio of component i (mole component i per mole inlet liquid)	[-]
y_i	Mole fraction of component i in gas phase	[-]

| Y_i | Molar ratio of component i (mole component i per mole inlet liquid) | [-] |
| Z_T | Height of packing | [m] |

Greek letters:

μ	Viscosity	[Pa.s]
ρ_L	Liquid density	$[\text{kg}.m^{-3}]$
ρ_G	Gas density	$[\text{kg}.m^{-3}]$
δ	Distance from interface	[m]
$\varphi(t)$	Age-distribution function	
σ_C	Critical surface tension	$[\text{N}.m^{-1}]$
σ_L	Surface tension of liquid	$[\text{N}.m^{-1}]$
$\emptyset$	Association factor for solvent ($\emptyset$= 2.6 for water)	
$\emptyset_L$	Liquid hold up in packed column	

CHAPTER (1)

INTRODUCTION

1.1. Background

All societies require energy services to meet basic human needs (e.g., lighting, cooking, space comfort, mobility, communication) and to serve productive processes. For development to be sustainable, delivery of energy services needs to be secure and have low environmental impacts. Sustainable social and economic development requires assured and affordable access to the energy resources necessary to provide essential and sustainable energy services. This may mean the application of different strategies at different stages of economic development. To be environmentally benign, energy services must be provided with low environmental impacts and low greenhouse gas (GHG) emissions. However, 85% of current primary energy driving global economies comes from the combustion of fossil fuels and consumption of fossil fuels accounts for 56.6% of all anthropogenic GHG emissions and GHG emissions associated with the provision of energy services are a major cause of climate change (Moomaw et al 2011). The The IPCC Fourth Assessment Report (AR4) concluded that "Most of the observed increase in global average temperature since the mid-20th century is very likely due to the observed increase in anthropogenic greenhouse gas concentrations." (IPCC, 2005).

The main reason why GHG has a great effect on global temperature is that GREENHOUSE GASES such as carbon dioxide (CO_2) absorb heat (infrared radiation) emitted from Earth's surface. Increases in the atmospheric concentrations of these gases cause Earth to warm by trapping more of this heat.

Human activities—especially the burning of fossil fuels since the start of the Industrial Revolution—have great effect on increasing global average temperature. And since 1900, the global average surface temperature as shown in

figure (1.1) has increased by about 0.8 °C (1.4 °F). This has been accompanied by warming of the ocean, a rise in sea level, a strong decline in Arctic sea ice, and many other associated climate effects. Much of this warming has occurred in the last four decades. Detailed analyses have shown that the warming during this period is mainly a result of the increased concentrations of CO_2 and other greenhouse gases. Continued emissions of these gases will cause further climate change, including substantial increases in global average surface temperature and important changes in regional climate. The magnitude and timing of these changes will depend on many factors, and slowdowns and accelerations in warming lasting a decade or more will continue to occur. However, long-term climate change over many decades will depend mainly on the total amount of CO_2 and other greenhouse gases emitted as a result of human activities.
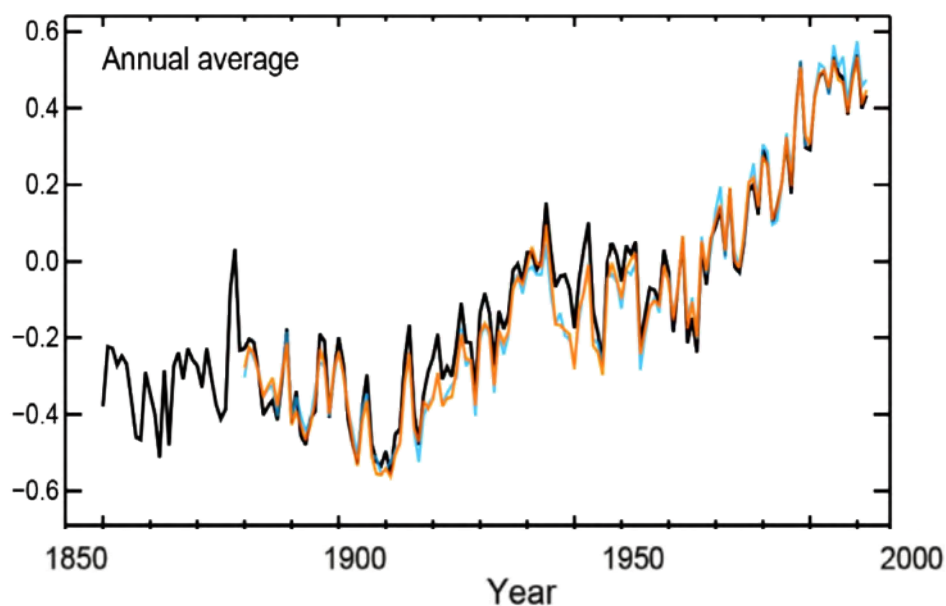
Figure 1.1: Earth's global average surface temperature Source: IPCC AR5, data from the HadCRUT4 dataset (black)

The atmospheric concentration of CO_2 has increased by 40% Since pre-industrial times as can be seen in figure (2.1) , methane has increased by about 150%, and nitrous oxide has increased by roughly 20%. More than half of the increase in CO_2 has occurred since 1970. Increases in all three gases contribute to warming of Earth, with the increase in CO_2 playing the largest role.
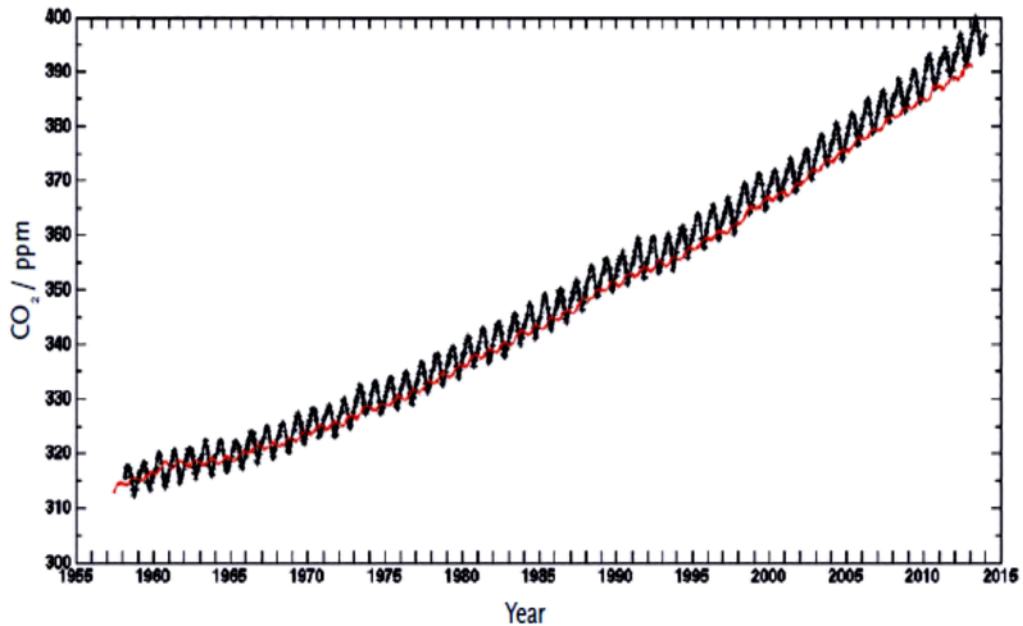
Figure 1.2:   Measurements of atmospheric CO2 since 1958 Source: : IPCC
AR5,Scripps CO2 Program

Adding more CO_2 to the atmosphere will cause surface temperatures to continue to increase. As the atmospheric concentrations of CO_2 increase, the addition of extra CO_2 becomes progressively less effective at trapping Earth's energy, but surface temperature will still rise.

So one of the biggest challenges our modern society has to face is the preservation of the environment combined with a growing world energy demand driven by the fast increase of the world population and the expectation of a higher standard of living. To face these challenges, it is necessary to re-evaluate and improve our way of dealing with energy. Reducing energy wastes on the production side as well as on the end-use side and promoting renewable energies are the best solutions towards sustainable energy systems. A third solution that could be rapidly applied at a large scale is to reduce the impact of the energy transformation steps on the environment. This can be accomplished by reducing the amount of emitted greenhouse gases, especially CO_2 which is the most widely produced greenhouse gas.

3

There are primarily three alternatives to lowering CO_2 emissions to the atmosphere:

1) use alternative energy sources to meet energy demands while lowering CO_2 emissions;

2) lower the consumption of energy that produces CO_2;

3) capture and sequester CO_2 before it is emitted to the atmosphere.

1.2. Capture technology of CO_2

The CO_2 produced as part of the energy conversion process is captured prior to being released to the atmosphere and subsequently stored. CO_2 capture and storage is a viable solution for CO_2 wherever fossil fuels are used as an energy source and opportunities for storage exist

There is several technology available in capturing CO_2(Wang et al ,2011) these include

- Chemical and physical absorption
- Adsorption
- Membrane separation
- Cryogenic separation

1.2.1. Adsorption

Adsorption is a physical process that involves the attachment of a gas or liquid to a solid surface. The adsorbent is regenerated by the application of heat (temperature swing adsorption, TSA) or the reduction of pressure (pressure swing adsorption, PSA). Adsorbents which could be applied to CO_2 capture include activated carbon, alumina, metallic oxides and zeolites (IEA GHG, 1993, Zhao et al, 2007). Current adsorption systems may not be suitable for application in large-scale power plant flue gas treatment. At such scale, the low adsorption capacity of most available adsorbents may pose significant challenges. In addition, the flue gas streams to be treated must have high CO_2 concentrations because of the generally low selectivity of most available adsorbents. For instance, zeolites have a stronger affinity for water vapor. (IEA 2004, IEA 2007, Zhao et al, 2007)
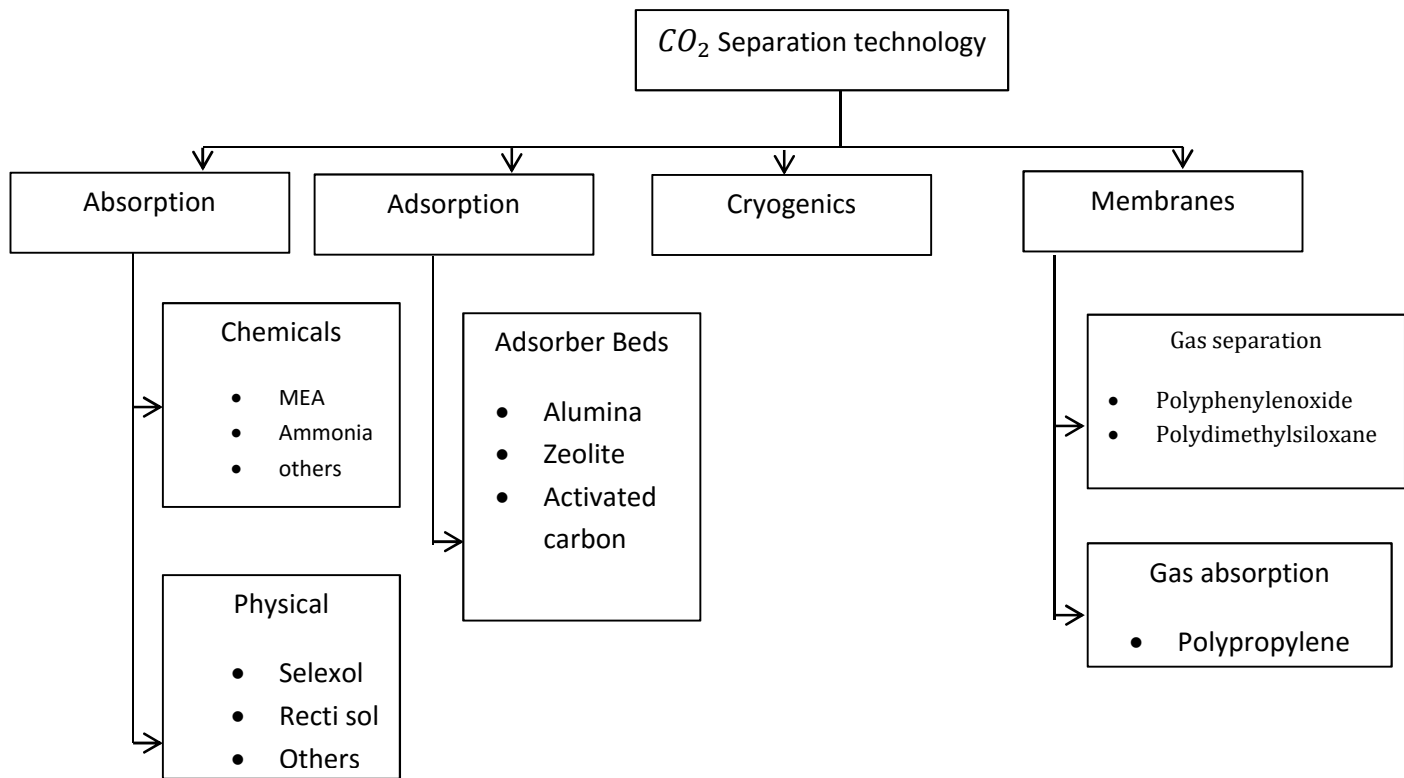
1.2.2 .Physical absorption

This involves the physical absorption of CO_2 into a solvent based on Henry's law. Regeneration can be achieved by using heat, pressure reduction or both. Absorption takes place at high CO_2 partial pressures. As such, the main energy requirements originate from the flue gas pressurization. Physical absorption is therefore not economical for gas streams with CO_2 partial pressures lower than 15 vol% (Chakravati et al, 2001, IEA, 2004). Typical solvents are Selexol (dimethyl ethers of polyethylene glycol) and Rectisol (methanol) (IEA GHG, 1993).

1.2.3 .Cryogenics separation

Cryogenics separation separates CO_2 from the flue gas stream by condensation. At atmospheric pressure, CO_2 condenses at -56.6°C (IEA GHG, 1993). This physical process is suitable for treating flue gas streams with high CO_2 concentrations considering the costs of refrigeration. This is also used for CO_2 capture for oxyfuel process.

1.2.4. Membrane absorption

When membranes are used in gas absorption, membranes act as contacting devices between the gas stream and the liquid solvent. The membrane may or may not provide additional selectivity. These offer some advantages over the conventional contacting devices such as packed columns as they are more compact and are not susceptible to flooding, entrainment, channeling or foaming. They, however, require that the pressures on the liquid and gas sides are equal to enable CO_2 transport across the membrane.

Their separation efficiency depends on the CO_2 partial pressure. As such, they are suitable for high CO_2 concentration applications (well above 20 vol%) such as flue gas streams from oxyfuel and IGCC processes. (IEA GHG 1993, IPCC, 2005).

1.2.5 .Membrane-based separations

In membrane-based separation, selectivity is provided by the membranes themselves. These usually consist of thin polymeric films and separate mixtures based on the relative rates at which constituent species permeate. Permeation rates would differ based on the relative sizes of the molecules or diffusion coefficients in the membrane material. The driving force for the permeation is the difference in partial pressure of the components at either side of the membrane. However, the selectivity of this separation process is low and thus a smal fraction of CO_2 is captured. In addition, the purity of the captured CO_2 is low for the same reason (IEA, 2004, IEA GHG, 1993). Multistage separation is employed to capture a higher proportion of CO_2 incurring extra capital and operating cost (Chakravati et al, 2001, IEA, 2004, IEA GHG, 1993).

1.2.6. Chemical absorption

Chemical absorption involves the reaction of CO_2 with chemical solvent to form a weakly bonded intermediate compound which may be regenerated with the application of heat producing the original solvent and a CO_2 stream (IPCC, 2005). The selectivity of this form of separation is relatively high. In addition, a relatively pure CO_2 stream could be produced. These factors make chemical absorption well suited for CO_2 capture for industrial flue gases.

Since absorption has such advantages as large capacity, high efficiency and good industrial performance, it always has been favored by researchers. Existing CO2 removal plants operate with different solvents which can be grouped together in two families:The **amine solvent** ; and the ***The hot potassium carbonate solvent***

Alkanolamines are most widely used as the chemical solvent in gas treating process for acid gas removal in the natural gas and petroleum processing industries. The common amine based solvents used for the absorption process are monoethanolamine (MEA), diethanolamine (DEA) and methyldiethanolamine (MDEA) that reacts with the acid gas (CO_2 and H2S) to form a complex or bond. H_2S, CO_2 and SO_2 are termed as acid gases since they dissociate to form a weak acidic solution when they come into contact with water or an aqueous medium. These amines are known as weak organic bases.
Alkanolamines can be divided into three groups:

(1) Primary amines whose members include monoethanol amine (MEA), diglycolamine (DGA);Using the primary amine monoethanolamine (MEA), is an efficient CO_2 capturing method. However, MEA has a high vapour pressure, and hence, it is not suitable for low pressure operations due to possible evaporation losses. Moreover, MEA is highly corrosive and may undergo severe degradation in presence of CO_2

(2) Secondary amines whose members include diethanolamine (DEA), di isopropylamine (DIPA); represent alternatives to MEA . DEA is more resistant to solvent degradation and corrosion than MEA, whereas DIPA has lower steam regeneration requirement than MEA.

(3) Tertiary amines whose members include triethanolamine (TEA) and methyl diethanolamine (MDEA).

In this way, recovery rates of 95-98% are possible.

In comparison to the benchmark amine-based solvents (in particular monoethanolamine (MEA)), potassium carbonate has a number of advantages such as low heat of absorption, low cost, less toxic and solvent losses, no thermal and oxidative degradation, without the formation of heat-stable salts . The challenge associated with using k_2CO_3 is the slow reaction rate of absorption, resulting in poor mass transfer .Moreover, for post-combustion capture, the absorption process is desired to run at flue gas conditions such as normal pressure and relatively low temperature .The absorption rate would be worse than that in Benfield process. Therefore, the possibility of rate enhancement by use of promoters is of significant interest to improve the CO_2 mass transfer rates .

Amine solvents have long been used for CO_2 absorption; however, marked improvements are being made in both the formulation of new solvents, and modifications to the process to increase efficiency (Devries, Nicholas P ,2014). One example is the use of an 8 M piperazine (PZ) solution, which has twicevthe rate of CO_2 absorption and 1.8 times the intrinsic working capacity of traditional 30 wt%MEA. Since 2001 the reboiler heat duty for amine scrubbing has improved from 5.5 MJ/tonne CO_2 to as low as 2.6 MJ/tonne CO_2 in 2012 (Boot-Handford et al., 2014). Many companies use proprietary solvents as well as advanced heat integration techniques to further decrease their parasitic energy loss.

Ionic liquids (ILs) are a recent introduction to the CO_2 capture conversation, as a potential replacement for traditional amines (Devries, Nicholas P ,2014). A major issue that has been associated with CO_2 removal by amine circulation has been solvent degradation and the various problems it presents.

Degradation can cause solvent loss, corrosion, fouling and foaming. ILs have negligible vapor pressure, tunable chemical properties, low regeneration energy and a wide liquid temperature range. They function with limited water, which decreases energy requirements. Certain Ils comprised of amine or carboxylate functional groups are preferential for CO_2 capture under low pressure, such as postcombustion capture. The main drawback to ILs is they are highly viscous, expensive, tend to not be stable to water vapor and flue gas impurities and have low CO_2 absorption capacity per unit of mass (Kenarsari et al., 2013).

Also a new class of solvent is CO_2 binding organic liquids (Devries, Nicholas P, 2014). Which is a mixture of alcohols and organic bases that reversibly react with CO_2. In amine based CO_2 capture, the efficiency is tied to the amount of water in the process. Binding organic liquids (BOLs) can be used in the presence of water without adverse effects, but do not require large amounts. CO_2 BOLs have 2 to 3 times higher capacity than aqueous alkanolamines. The difference in chemistry is the CO_2 is bound as an alkylcarbonate salt instead of a carbamate based salt. Early CO_2 BOLs had potential, but the vapor pressure was too high. Second generation BOLs are nonvolatile single component systems that react reversibly with CO_2. This resulted in a lower cost and decreased solvent regeneration energy; the stripping of CO_2 from these liquids consumes low energy. CO_2 BOLs have potential, but further investigation is needed to explore the potential of these solvents for real CO_2 capture applications (Kumar et al., 2014).

Another class of solvents for CO_2 capture application is amino acid salts. They are being investigated because of their fast reaction kinetics, high achievable cyclic loadings, good stability towards oxygen and favorable CO_2 binding energy. One advantage of using theses salts is for high CO_2 loading, precipitation will occur. Either bicarbonate salt or the neutral amino acid can precipitate out, resulting in increased absorption capacity. The majority of the testing done is on the laboratory scale and performance has been dependent on individual amino acid salts tested.

1.3 Problem formulation

Modeling of reactive absorption has been studied intensively in literature by numerous researchers ,Pacheco and Rochelle (1998) developed a general frame work that can be used to model the interfacial heat and mass transport processes that take place during reactive absorption when both rate and equilibrium controlled reactions take place in the liquid phase. And Mandala et al (2001) develop a model to describe CO_2 absorption into aqueous blends of methyldiethanolamine (MDEA) and monoethanolamine (MEA), as well as 2-amino-2-methyl-1-propanol (AMP) and monoethanolamine (MEA). Bolhàr-Nordenkampf et al (2004) implement a rate-based algorithm in Aspen (RATEFRACTM) to yield a predictive tool for MDEA acid gases scrubbing processes and a new enhancement model is developed to account for the chemical reactions in the liquid phase. Qian et al (2009) obtained analytical expression of the concentration distribution of CO_2 as a function of time and penetration depth in liquid film, and that of the gas-liquid mass transfer coefficient in RPB based on Higbie's penetration theory. A mathematical model is developed in this work to quantitatively describe the gas-liquid mass transfer process with reversible reactions in a RPB.

Mudhasakul et al, (2013) study a mixed solvent composed of MDEA and piperazine, called a-MDEA, In the first part of this study, an Aspen Plus simulation model of an existing commercial CO_2 capture process called the Acid Gas Removal Unit using a-MDEA was developed in order to validate its accuracy against plant design data and actual data. In the second part of the study, the validated simulation model in the first part was used to carry out sensitivity analyses.

Several kind of solvent has been considered in the past ,the most experienced one is amine family, and it was conclude that Amine absorption suffers from several drawbacks like corrosiveness, instability in the presence of oxygen, high energy consumption, especially during desorption, and high liquid losses due to evaporation of the solvent in the stripper. In addition, also the occurrence of flooding and entrainment of the absorption liquid may occur and limits the process as the gas and the liquid streams cannot be controlled independently. However, N-Methyldiethanolamine (MDEA) which is a tertiary amine whose

amino group is incapable of reacting with CO_2 and it is alkaline and so is an excellent sink for protons produce by CO_2 hydrolysis has a number of properties which make it attractive for CO_2 removal (BULLIN et al 2006); high solution concentration (up to 50-55 wt%) ,high acid gas loading,low corrosion even at high solution loadings,slow degradation rates ,lower heats of reaction ,and low vapor pressure and solution losses.

The primary disadvantages are ;slow reaction rate with CO_2,Tendency to foam at high concentration, and higher cost.The slow reaction rate can be overcome to a significant degree by adding a promoter; Amino-acid salt solutions provide an interesting promoter for CO_2 capture from flue gases. Because of it's distinguishing features which are; fast reaction kinetics, high achievable cyclic loading, good stability towards oxygen, favourable binding energy

Generally, a high reaction rate is important to reduce the size and hence the capital costs of an absorber, while a low pKa is of importance to minimize the energy requirement in a desorber. Based on these criteria, salts of L-proline, sarcosine and glycine, which combine a relatively high reaction rate constant with a relatively low pKa value, are promising solvents for CO_2 capture.

Packed columns are widely used for the separation of CO_2 from process gas streams in the chemical and petroleum industries. This is a well-developed technology and is currently the most preferred process approach for the CO_2 capture from power plant flue gases (Idem and Tontiwachwuthikul, 2006). However, packed-bed absorption columns are known to suffer from various operational problems including high gas phase pressure drop, liquid channeling and flooding of the packing materials resulting in a poor gas–liquid contact.

In order to achieve high CO_2 capture efficiency, there is a need for improved design of packed-bed absorption columns and optimization of operating conditions, which can be facilitated via the use of advanced process models for reactive absorption. In this thesis the performance of MDEA as solvent will be studied when it is promoted with potassium glycinate at packed bed column.

1.4 Objectives of this study

Following the work of the previous researchers the objectives of this work are:

- Creating a mathematical model of reactive absorption of CO_2 into promoted MDEA with piperazine at packed column. Data for thermodynamic properties and chemical reactions used in the simulation were gleaned from previous experimental studies on the MDEA-PZ-CO_2 system.

- Perform validation of the mathematical model by comparing the predicted results with actual data of an existing natural gas sweetening process in Thailand called Acid Gas Removal Unit (AGRU) which also promoted MDEA with piperazine.

- Develop a simulation model with an amino acid promoter, potassium glycinate, instead of piperazine in the same gas feed condition and column configurations.Study theoretically the performance of the column and assessing the effect of various process variables such as potassium glycinate concentration, solvent feed flow rate, feed temperature of both gas and liquid stream, and finally the pressure of the absorber on CO_2 absorptive capability.

The developed model can help in the process of designing a packed column in industrial scale and also in optimization of operating conditions.

CHAPTER 2
LITERATURE REVIEW

CO_2 capture in amine solvents is based on the reversible transfer of CO_2 from the gas phase into the liquid phase where it reacts with the amine solvent(reactive absorption). There are three main physical or chemical phenomena take place in the CO_2 capture process (Grégoire L,2013):

- Hydrodynamics: amine solvent and flue gas flow in counter current through the column packing. Their intimate contact is maximized by using appropriate column packing in order to increase the specific interfacial area between gas and liquid and thus to enhance the CO_2 transfer.
- Mass transfer: at the phase interface, CO_2 is transferred from the flue gas into the amine solvent. However, the mass transfer may be slowed down due to physical diffusivity limitations.
- Chemical reaction: CO_2 chemically reacts with the amine solvent, which enhances the CO_2 mass transfer. However, the reaction may be slowed down by chemical kinetics limitations.

In the present section, these three phenomena are first discussed separately and the different modeling approaches are presented in each case. Then, it is presented how these models can be combined to simulate the reactive absorption (respectively desorption) in mass transfer columns.

2.1 Physical Mass Transfer

There are basically two ways to deal with the modeling of mass transfer phenomena in the case of reactive absorption:

- Equilibrium assumption: this modeling approach considers that mass transfer columns are composed of successive equilibrium stages. On each stage, a perfect equilibrium is achieved, so that the liquid phase flowing to the lower stage is in equilibrium with the gas rising to the upper stage. Mass and heat transfer limitations are neglected.

- The rate-based approach: this method implies the rigorous calculation of mass transfer rates in the column at non-equilibrium conditions. Heat and mass transfer limitations are taken into account.

Although the first approach is computationally less intensive, it tends to overestimate the efficiency of the absorption (respectively desorption) process since mass and heat transfer limitations are neglected (Grégoire L,2013)..

On the contrary, the rate-based approach is based on theoretical assumptions and the drawbacks due to more intensive computational calculations are usually compensated for by an increased model precision. The rate-based modeling is currently the standard state-of-the-art method for CO_2 capture modeling. It requires a good characterization of the fluid properties, as well as of the column hydrodynamics (Grégoire L,2013)..

In this section, the main mass transfer models for rate-based calculations are presented.and a discussion of the different theories is necessary, since it defines the choice of mass transfer used in this work.

2.1.1 The film model

In the film model, we imagine that all of the resistance to mass transfer is concentrated in a thin film, or layer, adjacent to the phase boundary. Also that transfer occurs within this film by steady-state molecular diffusion alone and that outside this film, in the bulk fluid, the level of mixing or turbulence is so high that all composition gradients are wiped out (see Figure 2.1). Mass transfer occurs through this film essentially in the direction normal to the interface. That is, any constituent molecular diffusion or convection in any flow parallel to the surface due to composition gradients along the interface is negligible in comparison to the

mass transfer fluxes normal to the interface (Taylor and Krishna, 1954). The thickness of this hypothetical film is in the range 0.01-0.1 mm for liquid-phase transport and in the range 0.1-1 mm for gas-phase transport.
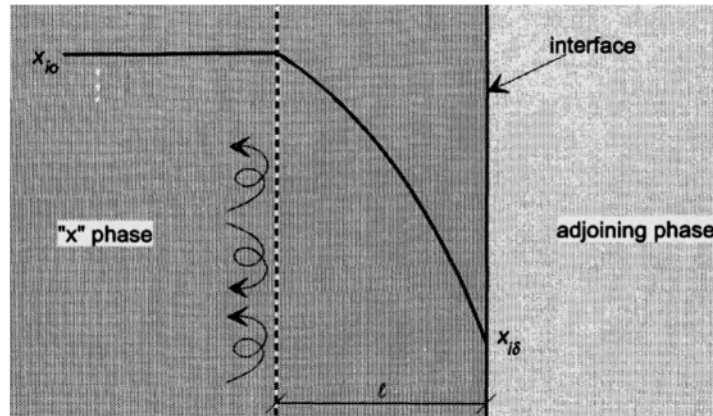
Figure 2.1: Film model for transfer in phase x.

As shown in figure 2.1Turbulent eddies wipe out composition gradients in the bulk fluid phase. Composition variations are restricted to a layer (film) of thickness ℓ adjacent to the interface.

Having made the appropriate simplifications to the hydrodynamics, the relevant differential equations describing the molecular diffusion process in the diffusion layer may now be solved. The diffusion process is fully determined by

1. The one-dimensional steady-state of forms of differential mass balance(Eqs. 2.1 and 2.2)

In terms of the component molar fluxes Ni as

$$\frac{\delta c_i}{\delta t} + \nabla . N_i = 0 \qquad (2.1)$$

The differential balance expressing conservation of total moles of mixture is obtained by summing Eqs. 2.1 For all components to give

$$\frac{\delta C_t}{\delta t} + \nabla . N_t = 0 \qquad (2.2)$$

- And the one dimensional form for the steady state case

$$\frac{dN_i}{dr} = 0 \qquad \frac{dN_t}{dr} = 0 \tag{2.3}$$

Showing that Ni and Nt are r invariant.

2. The constitutive relations
   - The force acting on species / per unit volume of mixture tending to move the molecules of species i is ciRTdi, where di is related to the relative velocities (ui — uj), by (Eqs. 2.4)

$$d_i = -\sum_{j=1}^{n} \frac{x_i x_j (u_i - u_j)}{D_{ij}}$$

$$= \sum_{j=1}^{n} \frac{(x_i N_j - x_j N_i)}{c_t D_{ij}} \tag{2.4}$$

   - Matrix Representation of the Generalized Fick's Law, The set of (n − 1) equations, written in (n — 1) dimensional matrix notation

$$(J) = -c_t[D](\nabla x) \tag{2.5}$$

3. The determinacy condition (Eq. 2.1.6)

$$\sum_{i=1}^{n} v_i N_i = 0 \tag{2.6}$$

Where the vi can be considered to be determinacy coefficients

Analysis of film theory for physical absorption of CO_2, first the concentration of CO_2 in the liquid film is represented as function of time (t) and position (x)

$$D_A \frac{\partial^2 [A]}{\partial X^2} + R_A = 0 \tag{2.7}$$

And the boundary condition

$$[A] = [A]_i \qquad at\ X = 0 \tag{2.8}$$

16

$$[A] = [A]_B \quad at\ X = \infty$$

And for the special case of physical absorption of CO_2 with no chemical reaction and steady state with the associated boundary condition becomes

$$\frac{\partial^2 [CO_2]}{\partial X^2} = 0$$

$$[CO_2] = [CO_2]i \quad at\ X = 0 \qquad (2.9)$$

$$[CO_2] = [CO_2]_B \quad at\ X = \delta$$

Here, δ is the film thickness .Integration of this equation and evaluation of the boundary conditions leads to the following expressions for the concentration gradient of CO2 throughout the liquid boundary layer

$$[CO_2] = \frac{[CO_2]_B - [CO_2]_i}{\delta} X + [CO_2]_i \qquad (2.10)$$

Use of ficks law at the interface leads to the expression for the flux of CO_2 in equation (2.10). Comparing this to the empirical expression for mass transfer which state the flux should be proportional to the driving force for mass transfer and a liquid film mass transfer coefficient .Equation (2.11) shows the definition of the liquid mass transfer coefficient as derived from film theory

$$N_{CO2} = - D_{CO2} \frac{\partial [CO_2]}{\partial X} = \frac{D_{CO2}}{\delta} ([CO2]_i - [CO2]_B) \qquad (2.11)$$

$$k_l^0 = \frac{D_{CO2}}{\delta} \qquad (2.12)$$

2.1.2 Higbie penetration theory

Most of the industrial processes of mass transfer are unsteady state process. In such cases, the contact time between phases is too short to achieve a stationary state. This non stationary phenomenon is not generally taken into account by the film model. In the absorption of gases from bubbles or absorption by wetted-wall columns, the mass transfer surface is formed instantaneously and transient diffusion of the material takes place. Figure 2.3 demonstrates the

schematic of penetration model. Basic assumptions of the penetration theory are as follows:

1) Unsteady state mass transfer occurs to a liquid element so long it is in contact with the bubbles or other phase

2) Equilibrium exists at gas-liquid interface

3) Each of liquid elements stays in contact with the gas for same period of time
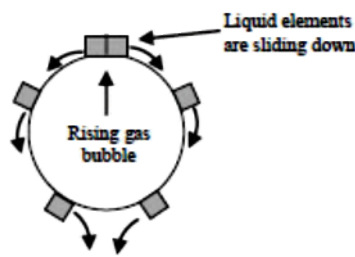
Figure 2.2: Schematic of penetration model.

Under these circumstances, the convective terms in the diffusion can be neglected and the unsteady state mass transfer of gas (penetration) to the liquid element can be written as:

$$\frac{\partial [A]}{\partial t} = D_{AB} \frac{\partial^2 [A]}{\partial X^2} \qquad (2.13)$$

The boundary conditions are:

$$t = 0, X > 0: [A] = [A]_B$$

$$t > 0, X = 0: [A] = [A]_i$$

$$t > 0, X = \infty: [A] = [A]_B.$$

The term $[A]_B$ is the concentration of solute at infinite distance from the surface and $[A]_i$ is the concentration of solute at the surface. The solution of the partial differential equation for the above boundary conditions is given by the following equation:

$$\frac{[A]_i - [A]}{[A]_i - [A]_B} = \mathrm{erf}\left[\frac{z}{2\sqrt{D_{AB}t}}\right] \qquad (2.14)$$

Where erf(x) is the error function defined by

$$\mathrm{erf}(x) = \frac{2}{\sqrt{\pi}}\int_0^x \exp(-X^2)dz \qquad (2.15)$$

If the process of mass transfer is a unidirectional diffusion and the surface concentration is very low ($[A]_B \sim 0$), the mass flux of component A, N_A [kg m–2 s–1], can be estimated by the following equation:

$$N_A = \frac{-\rho D_{AB}}{1 - [A]_B}\left(\frac{\partial[A]}{\partial X}\right)_{X=0} \approx -\rho\left(\frac{\partial[A]}{\partial X}\right)_{X=0} \qquad (2.16)$$

Substituting Equation (2.14) into Equation (2.15), the rate of mass transfer at time t is given by the following equation:

$$N_A(t) = \rho\sqrt{\frac{D_{AB}}{\pi t}}([A]_i - [A]_B) \qquad (2.17)$$

Then the mass transfer coefficient is given by

$$k_L(t) = \sqrt{\frac{D_{AB}}{\pi t}} \qquad (2.18)$$

The average mass transfer coefficient during a time interval *tc* is then obtained by integrating Equation (2.13) as

$$\bar{k}_{L,av} = \frac{1}{t_c}\int_0^{t_c} k(t)dt = 2\sqrt{\frac{D_{AB}}{\pi t_c}} \qquad (2.19)$$

Analysis of Higbie penetration theory for physical absorption of CO_2 results in elimination of the reactive term is equation (2.18).since the transient term is valid the equation is now a partial differential equation .Upon solution of this PDE and an analysis consistent with film theory, we end up with the

following expression for the mass transfer coefficient for Higbie penetration theory

$$k_l^o = \sqrt{\frac{4\,D_{CO2}}{\pi\tau}}$$ (2.20)

Penetration theory leads to a square root dependence of the mass transfer coefficient on the diffusion. This was first proposed by R. Higbie in 1935 and the theory is called Higbie's penetration theory and is consistent with experimental data which observes an order between 0.5 to 1 on the diffusion coefficient.

2.1.3 Surface Renewal Theory

For the mass transfer in liquid phase, Danckwert (1951) modified the Higbie's penetration theory. He stated that a portion of the mass transfer surface is replaced with a new surface by the motion of eddies near the surface and proposed the following assumptions:

1) The liquid elements at the interface are being randomly swapped by fresh elements from bulk

2) At any moment, each of the liquid elements at the surface has the same probability of being substituted by fresh element

3) Unsteady state mass transfer takes place to an element during its stay at the interface.
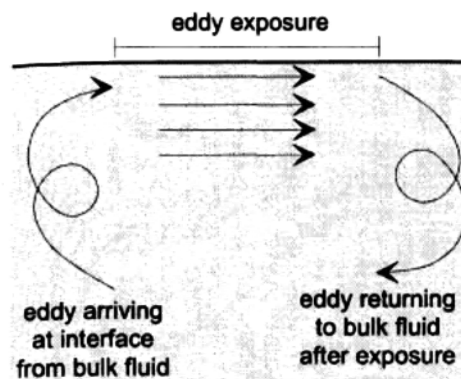
Figure 2.3: General representation of the surface renewal model.

20

An eddy arrives at the interface and resides there for randomly varying periods of time (Taylor and Krishna ,1954). During this period, there is plug flow of fluid elements. The bulk fluid is considered to be located at an infinite distance from the interface.

The basis for the Danckwerts (1951) surface renewal model is the idea that the chance of an element of surface being replaced with fresh liquid from the bulk is independent of the length of time for which it has been exposed. He proposed the following analytical form for the age-distribution function

$$\varphi\,(t) = s\exp(-st) \tag{2.21}$$

Where s has the physical meaning of the rate of surface renewal, and 1/s may be regarded as an "average lifetime" of surface elements.

Hence, average molar flux, $N_{A,av}$

$$N_{A,av} = (\,[A]_i - [A]_B)\sqrt{s\,\times\,D_{AB}} \tag{2.22}$$

The resulting expression for mass transfer coefficient

$$k_{L.av} = \sqrt{s\,\times D_{AB}} \tag{2.23}$$

In the penetration and surface renewal models, in which the surface film is replaced by bulk water after a fixed time interval, although between these periodic replacements molecular diffusion still determines the transfer between the film and the gaseous phase, the overall transfer velocity is a function of the time interval between film renewal events. Since this is shorter than the timescale of diffusion across the full width of the film, the film thickness itself is not a factor.

Toor and Marchello pointed out that the surface renewal model is valid only when the surface renewal is relatively rapid.

2.1.4 Eddy Diffusivity Theory

The major advantages of unsteady state theories are that they seem to predict the correct dependence of the diffusion coefficient on the mass transfer

coefficient. However, they introduce another variable (time) which complicates their use. King (1966) proposed a steady state theory that yields a square root dependence of the diffusion coefficient on the mass transfer coefficient .The physical concept is that there are convective eddies in the liquid phase which contribute to effective diffusion coefficient. At the interface, the effect of these eddies disappears and the dominant phenomena is diffusion. As the liquid depth increase, the effect of the eddies increase until they are the dominant phenomena at infinite liquid depth (Bishoni S,2000). This process is illustrated in figure 2.5 .Mathematically a material balance for eddy diffusivity theory is as follows:

$$\frac{d}{dx}\left[(D_{AB} + \varepsilon X^2)\frac{d[A]}{dX}\right] = 0 \tag{2.24}$$

Solving Eq (2.24) for the concentration gradient and applying Fick's law, we obtain the following expressions for the concentration profile and mass transfer coefficient using the eddy diffusivity theory

$$[A] = \frac{2}{\pi}([A]_B - [A]_i).\,arctan\left(\sqrt{\frac{\varepsilon}{D_{AB}}}.X\right) + [A]_i \tag{2.25}$$

$$k_l^0 = \frac{2}{\pi}\sqrt{D_{AB}\varepsilon} \tag{2.26}$$

Eddy diffusivity theory has the advantage of predicting the correct dependence of the diffusion coefficient on the mass transfer coefficient without the added computation complexity of unsteady state theory. Glasscock (1990) has shown the absorption with chemical reaction predictions from eddy diffusivity theory is comparable to surface renewal and penetration theory with 5 %.
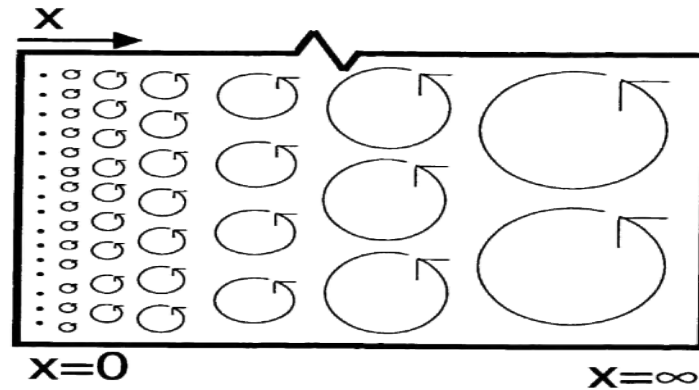
Figure 2.4: eddy diffusivity theory

2.1.5 The Film – Penetration Theory

As the name suggests it is a combination of the Film and Penetration theories, and is similar to the surface renewal theory, the *film–penetration theory* adopts the unsteady–state molecular diffusion mechanism as the means of mass transport through the film or the liquid element. An example for the derivation of the enhancement factor for the gas absorption with a simple first–order or pseudo first–order reversible reaction using this theory can be found in literature.

This theory assumes that the entire resistance to mass transfer resides in a film of fixed thickness δ. Eddies move to and from the bulk fluid and this film. Age distribution for time spent in the film is of the Higbie or Danckwerts type
The governing system of equations is

$$\frac{\partial [A]}{\partial t} = D_{AB} \frac{\partial^2 [A]}{\partial X^2} \qquad (2.27)$$

With the initial and boundary condition

At t = 0; $[A] = [A]_B = 0$

At X = 0; $[A] = [A]_i$ (2.28)

At X = δ; $[A] = [A]_B = 0$

23

The solution is

$$\frac{[A]}{[A]_i} = \sum_{n=0}^{n=\infty} erfc \frac{(2nL+X)}{2\sqrt{D_{AB}t}} - \sum_{n=0}^{n=\infty} erfc \frac{[2(n+1)-X]}{2\sqrt{D_{AB}t}}$$

(2.29)

And mean mass flux

$$N_A = [A]_i \sqrt{\frac{D_{AB}}{\pi t}} \left\{ 1 + 2\sum_{n=1}^{n=\infty} \exp(-\frac{n^2 L^2}{D_{AB}t}) \right\}$$

(2.30)

2.2 Mass transfer with chemical reaction

Several simplifying assumptions lead to asymptotic behavior of the enhancement factor .These assumptions are very valuable when estimating the enhancement factor and, in some cases, are extremely accurate (Bishoni S,2000).

We are going to discuss about the case of pseudo first order and when it is a valid assumption.

2.2.1 Pseudo First order Case

- Irreversible Reactions

Pseudo first order behavior assumes the overall reaction kinetics to be first order.

Take component A and B, with A react and absorbed in B. Making the assumption that the concentration of B is constant over the length of the liquid boundary layer, we can combine B concentration with the rate constant to obtain a pseudo first order rate expression.

(2. 31)

$$\frac{d^2[A]}{dx^2} - k_1[A] = 0$$

Where k_1 is the pseudo first order rate constant. With appropriate boundary conditions, this expression can be integrated to obtain the following expression for the concentration of A in the boundary layer. This case is discussed in Danckwerts (1970).

$$[A] = \frac{1}{sinh\sqrt{M}}\left[[A]_B \ sinh\left(x\sqrt{\frac{k_1}{D_A}}\right) + [A]_i \ sinh\left(\frac{D_A}{k_L^o} - x\right)\sqrt{\frac{k_1}{D_A}}\right] \tag{2.32}$$

Where:

M (Hatta Number) $= \frac{D_A k_1}{k_l^{o^2}}$

k_l^o (Liquid film mass transfer coefficient) $= \frac{D_A}{\delta}$

Applying Fick's law at the gas liquid interface, the following expression is obtained for the flux under pseudo first order conditions:

$$N_A = k_l^o\left([A]_i - \frac{[A]_B}{cosh\sqrt{M}}\right)\frac{\sqrt{M}}{tanh\sqrt{M}} \tag{2.33}$$

As the rate of reaction and the Hatta number increase, most of the reaction occurs in the liquid film and $[A]_B$ approaches 0. The tanh contribution approaches one and we obtain the following expression

$$N_A = k_l^o \ \sqrt{M} \ [A]_i \tag{2.34}$$

So the enhancement factor is equal to the square root of the Hatta number

Substituting the Hatta number into this expression (equation 2.34), the mass transfer coefficient inside and outside the square root term cancel. We obtain the result that the flux is independent of the liquid film mass transfer coefficient and directly related to the square root of the amine concentration and the rate constant.

$$N_A = \sqrt{k_1[B]D_{AB}} \ [A]_i \tag{2.35}$$

Since most amine reactions are first order in amine concentration and first order in CO_2 concentration (second order overall), the pseudo first order assumption is equivalent to assuming a constant amine concentration across boundary layer.

The criteria of Hatta number being greater than 5 is often satisfied with CO_2 reaction with amine (Bishoni S,2000).

- Reversible reactions

Consider the reversible reaction of A to form B ,We can write the reaction as first order reversible reaction with an associated equilibrium relationship:

$$A \quad \rightleftharpoons B \qquad (2.36)$$

$$r_A = k_1[A] - \frac{k_1}{K_{eq}}[B] \qquad (2.37)$$

$$K_{eq} = \frac{[B]}{[A]^*} \qquad (2.38)$$

So

$$r_{CO2} = k_1 ([A] - [A]_e) \qquad (2.39)$$

Where

$[A]_e$ Is the equilibrium concentration of A with the bulk phase concentration of B

The expression for the flux is

$$N_A = k_L^o ([A]_i - [A]_e)\sqrt{1 + M} \qquad (2.40)$$

In the case of absorption of CO_2 in amine for the solvent to be regenerable, the reaction of CO_2 with amines must be reversible.

The assumption of pseudo first order is valid if we consider the amine concentration along the length of the boundary layer to be constant. By material balance then, the concentration of amine product will be constant.

2.3 Reaction mechanism
2.3.1 Zwitterion Reaction Mechanism

Absorption of CO_2 by amines is often explained by the zwitterion mechanism, originally proposed by Caplow (1968) and reintroduced by

Danckwerts (1979). And the zwitterion is an ionic, but neutrally charged intermediate that is formed from the reaction of CO_2 with an amine.

The zwitterion mechanism for carbamate formation is a two-step process (Dugas, Ross Edward, 2009):

- First : the CO_2 reacts with the amine to form a zwitterion,
- Second: extraction of a proton by a base.

In the following example water acts as the base. For simplicity the zwitterion mechanism is shown with the usual convention of irreversible proton extraction

(2.41)

(2.42)
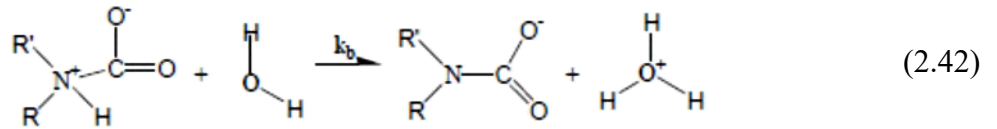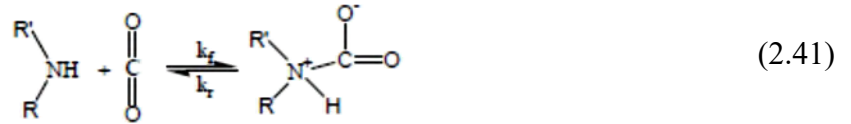
The two step zwitterion mechanism leads to the CO_2 absorption rate shown in Equation 2.43.

$$r_{CO2} = -\frac{[Am] + [CO_2]}{\frac{1}{k_f} + \frac{k_r}{k_f \sum k_b[B]}}$$

(2.43)

Bases can include the amine as well as H_2O and OH–. In some systems H_2O and OH– can contribute pronounced effects to the rate of reaction (Blauwhoff, Versteeg et al. 1983).

The reaction rate given by Eq. 2.43 exhibits a fractional order between one and two with respect to the amine concentration.

When deprotonation is almost instantaneous as compared to the reverse reaction in Eq. 2.41 ($k_r \ll k_b$ [B]) and zwitterion formation is rate-determining, Eq. 2.43 becomes:

$$r = -k_f[AM][CO_2]$$

(2.44)

There by suggesting that the reaction is of the first order with respect to both CO_2 and amine. When zwitterion deprotonation is rate-determining (kr >> kb(B)), Eq. 2.43 takes the form

$$r_{CO2} = -\frac{k_f}{k_r}[AM][CO_2]\sum k_b[B] \tag{2.45}$$

Similar to Eq. 2.43 the latter expression suggests a fractional reaction order between one and two with respect to the amine concentration

The zwitterion mechanism can also be solved with a reversible base protonation step. This causes the reaction in Equation 2.41 to be replaced by Equation 2.46

$$\tag{2.46}$$
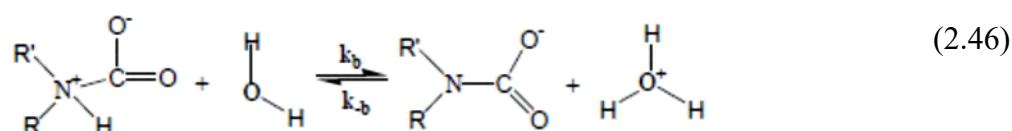
This leads to the following form of the rate equation, which now includes a driving force for the reversion of carbamate to amine and CO_2.

$$r_{CO2} = -\frac{[Am]}{\frac{1}{k_f}+\frac{k_r}{k_f\sum k_b[B]}}\left([CO_2] - \frac{\sum\frac{k_b}{K_{eq.b}}[AmCOO^-][BH^+]}{\sum k_b[Am][B]}\right) \tag{2.47}$$

The $K_{eq,b}$ term in Equation 2.47 is the overall equilibrium constant and is specific to the base pathway. For unloaded solutions, the reverse portion of Equation 2.47 can be ignored to produce the irreversible result of Equation 2.43. If the concentrations of the reactants and products are at equilibrium, the equilibrium constant will reduce the reversible term to $[CO_2]$ which will yield a zero for the rate of CO_2 formation.

2.3.2 Termolecular Reaction Mechanism

Contrary to the zwitterion mechanism, Crooks and Donnellan (1989) presented the Termolecular mechanism, which assumes the reaction proceeds via

a loosely bound complex. The complex and the reaction mechanism are shown in Equation 2.48

$$
\text{(2.48)}
$$

This mechanism coincides with the limiting case for the zwitterion mechanism where r k is much greater than $k_f \Sigma k_b [B]$. The rate of CO_2 absorption is identical to the zwitterion result shown in Equation 2.45.

It is theorized that most of the loosely bound complexes break up to produce reagent molecules again while a few react with a second molecule of amine or water to yield ionic products (Crooks and Donnellan 1989). The bond formation and charge separation occur in the second step.

Since both the zwitterion and termolecular reaction mechanisms allow for varying orders of the amine concentration, both can be fitted to experimental data. An equally effective representation of reaction rates should be possible using either mechanism.

2.3.3 Base-Catalyzed Hydration Mechanism

Donaldson and Nguyen (1980) reported that amines have a base-catalytic effect on the hydration of CO_2. This can be represented as:

$$R_3N + H_2O + CO_2 \xrightarrow{k'} R_3N^+H + HCO_3^- \qquad \text{(2.49)}$$
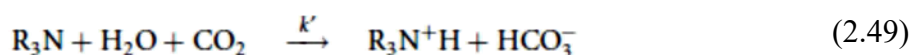
In aqueous solutions, an amine dissociation reaction may also occur

$$R_3N + H_2O \rightleftarrows R_3N^+H + OH^- \qquad \text{(2.50)}$$
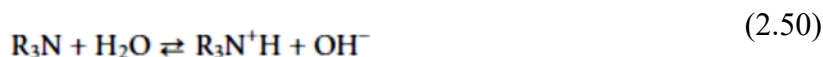
In principle, as reported by Jorgensen and Faurholt (1954), a direct reaction between CO_2 and tertiary amines still may occur at extremely high pH, thereby

resulting in monoalkylcarbonate formation. However, at pH values lower than 12, the rate of this reaction can be neglected .The total rate of all CO_2 reactions in an aqueous solution is thus represented by the sum of the reaction rates given by Eqs. 2.49 and 2.50

$$r_{ovrall} = [k_{H2o}(H_2O) + k_{OH^-}(OH^-) + k'(R_3N)](CO_2)$$
(2.51)

k_{obs} is given by:

$$k_{obs} = [k_{H2o}(H_2O) + k_{OH^-}(OH^-) + k'(R_3N)]$$
(2.52)

and k_{ap} by:

(2.53)
$$k_{ap} = [k'(R_3N)]$$

The base-catalysis reaction could also be explained by a zwitterion- type mechanism earlier:

(2.54)
$$R_3N + CO_2 \rightleftarrows R_3NCOO^-$$

(2.55)
$$R_3NCOO^- + H_2O \rightarrow R_3N^+H + HCO_3^-$$
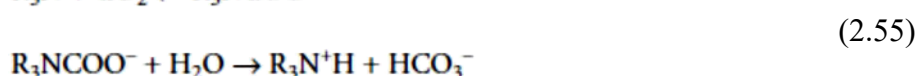
Eq 2.54 represents a reaction of the amine with CO_2 to form an unstable complex. Eq. 2.54 describes the homogeneous hydrolysis reaction in which water reacts with the zwitterion- type complex to yield bicarbonate

2.4 Mathematical models of Absorption Process

2.4.1 MDEA and CO2 and potassium glycinate Reaction System

- MDEA and CO2

In aqueous solutions, tertiary amines catalyze CO_2 hydrolysis to form bicarbonate ions and the protonated amine as was firstly proposed by Donaldson and Nguyen (Donaldson and Nguyen, 1980).

Tertiary amines have a high CO_2 loading capacity of 1 mol CO_2/mol amine. The reaction heat released in bicarbonate formation is lower than that of

carbamate formation, thus resulting in lower solvent regeneration costs. On the other hand, the formation of bicarbonate ions is relatively slow compared to the carbamate ion formation, so the kinetics of CO_2 removal by tertiary amines is generally slower than that for primary and secondary amines (Vaidya and Kenig, 2007).

In the reaction of tertiary amines with CO_2, a protonated amine and bicarbonate ions are produced. The reaction is consistent with a single step mechanism and water must be present for this reaction to proceed. According to Donaldson and Nguyen (Donaldson and Nguyen, 1980), the reaction can be described as a base catalyzed hydration of CO_2:

$$CO_2 + R_3N + H_2O \xleftrightarrow{k_2, K_1} R_3NH^+ + HCO_3^-$$ (2.56)
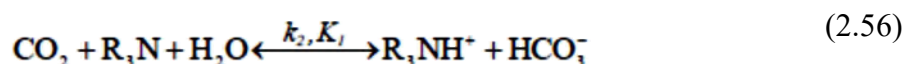
This most accepted mechanism goes through the formation of a hydrogen bond between the tertiary amine and water, thus weakening the O-H bond in water and increasing the reactivity towards CO_2. This reaction involves two bases: water, which catalyses CO_2 hydrolysis and the amine.

The following reactions also occur in aqueous solutions:

$$CO_2 + OH^- \xleftrightarrow{k_{OH}, K_2} HCO_3^-$$ (2.57)

$$HCO_3^- + OH^- \xleftrightarrow{K_3} CO_3^{2-} + H_2O$$ (2.58)

$$R_3NH^+ + OH^- \xleftrightarrow{K_4} R_3N + H_2O$$ (2.59)

$$2H_2O \xleftrightarrow{K_5} OH^- + H_3O^+$$ (2.60)
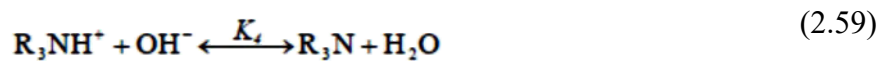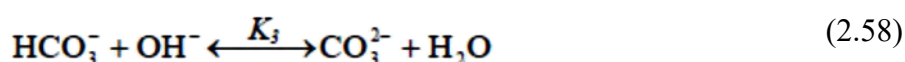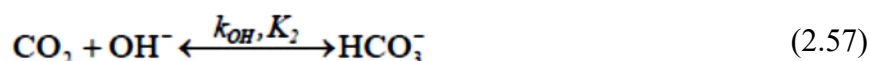
Reactions (2.56)-(2.57) take place in parallel with the finite rates which are described by the forward second order rate constants k_2 and k_{OH} and equilibrium constants K_1 and K_2. Reactions (2.58)-(2.60) are instantaneous as they involve only a proton transfer. Kinetics of the direct reaction of CO_2 with OH– is very fast and is firmly established (Pinsent and Roughton, 1956; Pohorecki and Moniuk, 1988) and its influence on the reaction rate should be considered very

carefully as it may have a significant contribution to the observed rate, especially at very low CO_2 partial pressure or short contact times (Kierzkowska-Pawlak and Chacuk, 2010).

Versteeg at al (1996) concluded that in a large number of studies of CO_2-MDEA system with an absorption technique, the influence of the OH– reaction with CO_2 is overestimated due to the presence of other negative charged ions like - 3 HCO and 2-3 CO. Littel et al (1992) and Moniuk et al (2000) claim that the effect of this reaction is negligible due to the low concentration of the hydroxide ions in the solution. According to the numerical simulation of Rinker et al(1995) and Glasscock and Rochelle (1989) only at low CO_2 concentrations, corresponding to low CO_2 partial pressure, the hydroxide reaction has the largest effect and must be taken into account in predicting the second order reaction rate constant k_2. As the partial pressure is increasing, the hydroxide becomes depleted in the boundary layer and MDEA has a major contribution to the absorption rate.

In the present work, the simplified kinetic model was applied which assumes that the main reaction (2.56) of CO_2 with MDEA is reversible and the contribution of reaction (2.57) on the mass transfer rate is negligible. The conditions for the absorption of CO_2 in MDEA solutions were selected in such a way as to ensure that the absorption occurs in the fast pseudo-first order reaction regime. After these assumptions, the total rate of CO_2 reaction in an aqueous solution of MDEA may be expressed as:

$$r_{ov} = k_2[R_3N]_B[CO_2] - \frac{k_2}{k_1}[R_3NH^+][HCO_3^-] \qquad (2.61)$$

At equilibrium the forward reaction is equal to the backward reaction so

$$k_2[R_3N]_B[CO_2]_e = \frac{k_2}{K_1}[R_3NH^+][HCO_3^-] \qquad (2.62)$$

So the reaction rate can expressed as

$$r_{MDEA} = k_2[R_3N]_B([CO_2] - [CO_2]_e) \qquad (2.63)$$

The overall reaction kinetic constant k_{ov} is defined as:

$$k_{ov} = k_2 [R_3N]_B \qquad (2.64)$$

Where $[R_3N]_B$ states for the bulk concentration of MDEA in the solution.

- *Reaction Kinetics Data*

The kinetics of the reaction of CO_2 with aqueous MDEA was widely investigated (Haimour et al.,1987; Jamal et al., 2006; Kierzkowska-Pawlak and Chacuk, 2010; Ko and Li, 2000; Littel et al., 1990; Moniuk and Pohorecki, 2000; Pani et al., 1997; Rinker et al., 1995) using several experimental techniques.

Kinetic data of the reaction between CO_2 and aqueous MDEA available in the literature are summarized in Table (2.1). There is a general agreement that tertiary amines act as catalysts for CO_2 hydrolysis reaction. However, there are still many discrepancies in the literature concerning the interpretation of kinetic data. This causes a relatively high difference in the forward rate constant of the MDEA-catalyzed reaction which is ranging from 1.44 m3 kmol s–1 (Haimour et al., 1987) to 5.15 m3 kmol s–1 (Jamal et al., 2006) at 293 K. Some of these discrepancies in the reported rate constants may be attributed to various experimental techniques and the assumptions made as well as the inconsistency of the physical data such as CO_2 solubility and diffusivity applied to interpret absorption rate data.

Table 2.1: reaction constant expression

Reference	T,K	[MDEA] kmol/m3	$k_2, \dfrac{m^3}{kmol.s}$
Haimour et al,1987	288-308	0-1.7	$8.741 \times 10^{12} \exp(-\dfrac{8625}{T})$
Rinker et al ,1995	293-423	0.83-2.5	$2.91 \times 10^7 \exp(-\dfrac{4579}{T})$
Pani et al ,1997	296-343	0.83-4.38	$2.07 \times 10^9 \exp(-\dfrac{5912}{T})$
Little et al ,1990	293-333	0-2.3	$1.2919 \times 10^9 \exp(-\dfrac{5760.56}{T})$
Ko and Li ,2000	303-313	1-2.5	$4.01 \times 10^5 \exp(-5400)$
Jamal et al,2006	293-383	0.4-3.2	$2.0 \times 10^9 \exp(-\dfrac{5797.8}{T})$
Moniuk and Pohorecki ,2000	293	0.83-2.5	5.7
Kierzkowska-Pawlak and Chacuk ,2010	293-333	0.84-1.706	$2.07 \times 10^9 \exp(-\dfrac{5912.7}{T})$
Kierzkowska-Pawlak et al ,2011	288-303	0.25-0.875	$1.78 \times 10^{10} \exp(-\dfrac{6441.9}{T})$

- *Reaction Equilibrium Data*

The following equilibrium constants were incorporated in the model

$$K_1 = \frac{[R_3NH^+][HCO_3^-]}{[H_2O][R_3N][CO_2]} \qquad (2.65)$$

$$K_2 = \frac{[HCO_3^-][H_3^+O]}{[CO_2][H_2O]^2} \qquad (2.66)$$

$$K_2' = K_2[H_2O] = \frac{[HCO_3^-][H^+]}{[CO_2][H_2O]}$$

$$K_3 = \frac{[CO_3^{-2}][H_3^+O]}{[HCO_3^-][H_2O]}$$

$$K_3' = K_3[H_2O] = \frac{[CO_3^{-2}][H^+]}{[HCO_3^-]}$$

(2.67)

$$K_4 = \frac{[R_3N][H_3^+O]}{[R_3NH^+][H_2O]}$$

$$K_4' = K_4[H_2O] = \frac{[R_3N][H^+]}{[R_3NH^+]}$$

(2.68)

$$K_5 = \frac{[H_3^+O][OH^-]}{[H_2O]^2}$$

$$K_5' = K_5[H_2O] = \frac{[H^+][OH^-]}{[H_2O]}$$

(2.69)

The temperature dependence of the equilibrium constants is expressed as

$$lnK_i = \frac{a_i}{T} + b_i \, lnT + c_i$$

(2.70)

Where a_i-c_i are constants. Values of these constants for reactions were taken from literature – see Table 3.2. These correlations are well established and have been utilized in many VLE models (Austgen et al., 1989).

It should be noted that not all reactions are equilibrium constants are independent. Only four equilibrium constant (K_2, K_3, K_4, K_5) is independent.And K_1 is obtained form the following equation (Edward B. Rinker, 1995)

$$K_1 = \frac{K_2}{K_4}$$

(2.71)

Table 2.2: Equilibrium constants

Parameter	a_i	b_i	c_i	Source
K_2	-12092.1	-36.7816	235.482	Edwards et al,1978
K_3	-12431.7	-35.4819	220.067	Edwards et al,1978
K_4	-4234.98	0	-9.4165	Posey,1996
K_5	-13445.9	-22.4773	140.932	Edwards et al,1978

Reaction (2.57) and (2.58) is assumed in equilibrium condition and from (2.64) and (2.65) the equilibrium concentration of CO2 in liquid phase is:

$$C_{CO2,e} = \frac{K_3[HCO_3^-]^2}{K_2[CO_3^-]^2} \qquad (2.72)$$

- Amino acid and CO_2 system
  - ➤ Solvent preparation

salts of amino acids are used for the absorption of CO_2. These salts are obtained by neutralising the amino acid with potassium hydroxide. When a pure amino acid, with the overall formula HOOC-R-NH2, is dissolved in water, the following equilibria are established(Brouwer et al):

$$\underset{\text{low }pH}{\text{HOOC-R-NH}_3^+} \quad \overset{\text{-H}^+}{\longleftrightarrow} \quad \underset{\text{neutral - mildly acid }pH}{\text{-OOC-R-NH}_3^+} \quad \overset{\text{-H}^+}{\longleftrightarrow} \quad \underset{\text{high }pH}{\text{-OOC-R-NH}_2} \qquad (2.73)$$
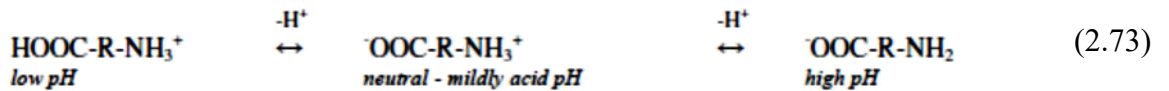
It is thus seen that in solution the neutral molecule takes the form of a dipole, because the carboxylic group loses a proton while the amine group is protonated. When the amino acid is reacted with potassium hydroxide, a proton is removed from the –NH3 + group and a potassium salt solution is obtained:

$$\text{-OOC-R-NH}_3^+ + \text{KOH} \longrightarrow \quad \text{K}^+ + \text{-OOC-R-NH}_2 + \text{H}_2\text{O} \qquad (2.74)$$
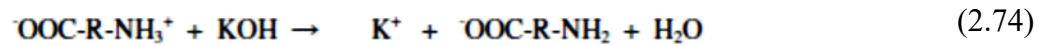
The K-salt is the active component, which reacts with CO_2 like "normal" amines via the NH_2-group. The solubility is greatly enhanced due to the neutralisation.

  - ➤ Reactions with CO_2

CO2 reacts with potassium glycinate forming a zwitterion that is subsequently deprotonated by a base present in solution (Portugal et al,2007).

- Formation of the potassium glycinate zwitterion:

$$H_2N - CH_2 - COO - K^+ + CO_2 \underset{k_{-1}}{\overset{k_2}{\rightleftharpoons}} {}^-OOC^+H_2N - CH_2 - COO^-K^+ \qquad (2.75)$$
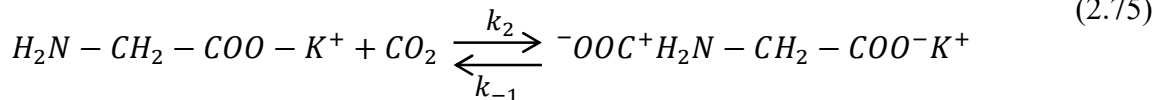
- Removal of a proton by a base:

$$^-OOC^+H_2N - CH_2 - COO^-K^+ + B_I \xrightarrow{k_{Bi}} {}^-OOCHN - CH_2 - COO^-K^+ + B_IH^+ \qquad (2.76)$$

36
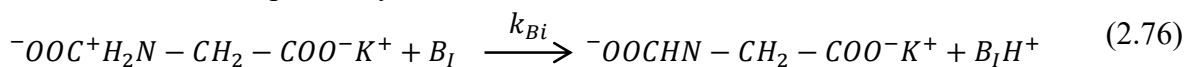
Where B_I are the bases present in solution able to deprotonate the zwitterion. In amino acid salt solutions, these bases are H_2O, OH− and the amino acid salt $H_2NCH_2COO^-K^+$ (Blauwhoff et al., 1984).

Assuming quasi-steady-state condition for the zwitterion concentration and since the second proton transfer step can be considered irreversible, the overall reaction rate, $-r_{CO_2}$, can then be obtained:

$$r_{CO_2} = \frac{k_2}{1+\frac{k_{-1}}{\sum_i k_{Bi}[B]_i}}[S][CO_2]_B \tag{2.77}$$

Where $[S]$ is the concentration of the amino acid salt and $[CO_2]_B$ is the concentration of carbon dioxide in the liquid. Limiting conditions lead to simplified reaction rate expressions that are well described in literature (Derks et al., 2006; Kumar et al., 2003a).

The deprotonation of the zwitterion is relatively fast when compared to the reversion rate of CO2 and the amine $(k_{-1}/\sum_i k_{B_i}C_{B_i} \ll 1)$Eq. (2.77) is then reduced to

$$r_{CO_2} = k_2[S][CO_2]_B \tag{2.78}$$

And k_2 is

$$k_2 = 2.81 \times 10^{10} \exp(-\frac{58\ 00}{T})m^3mol^{-1}S^{-1} \tag{2.79}$$

2.4.2 Reactive absorption models

As already mentioned, fluid hydrodynamics, chemical reactions and mass transfer are strongly inter-dependent phenomena. In particular, the transfer coefficients determined from a mass-transfer model may be used to characterize the physical absorption of CO_2 in the amine solvent, but they do not consider the chemical reaction of CO_2 with the amine. However, chemical reactions taking place at the gas-liquid interface strongly enhance the reactive absorption. Considering mass transfer as independent of chemical equilibria would only lead to unreliable results (Léonard, Grégoire, 2013).the main method to include chemical reactions in the rate-based mass transfer models is by concluding the enhancement factor in calculating the rate of mass transfer.

$$N_A = k_L . a . ([A]_i - [A]_B)E \qquad (2.80)$$

- N_A is the mass transfer of component A (kmol/s)

- k_L is the overall mass transfer coefficient (m/s)

- a is the interface area (m²)

- $[A]_i$ is the concentration of component A at the interface

- $[A]_B$ is the concentration of component A in the bulk (kmol/m³)

- E is the enchancement factor (-)

This enhancement factor depends on the reaction kinetics and on the diffusion coefficients of the components implied in the reaction. Many studies have been performed to evaluate the enhancement factor in function of the Hatta number, a dimensionless number that compares the chemical reaction kinetics with the pure physical mass transfer. Considering a first-order reaction between absorbed component A and solvent component B taking place in the liquid phase, the Hatta number can be defined as:

$$Ha = \frac{\sqrt{D_{A,L} k [B]}}{k_L^o} \qquad (2.81)$$

- $D_{A,L}$ is the diffusion coefficient of component A in the liquid phase (m²/s)
- k is the kinetic constant of the chemical reaction between absorbed component A and solvent component B (m³/kmol.s)
- $[B]$ is the concentration of component B in the liquid bulk (kmol/m³)
- k_L^o is the physical mass transfer coefficient (m/s)

Based on the reaction kinetics and on the mass transfer model, different expressions for the enhancement factor have been proposed. According to Dubois (2013), the mass transfer model has no significant influence on the numerical value of the enhancement factor. Faramarzi et al (2010) have compared three expressions of the enhancement factor based on the film model for the reactive

absorption of CO2 in MEA. These expressions are listed in table 2.3(Grégoire L , 2013).

In the case of a pseudo-first order reaction, the enhancement factor reduces to the Hatta number. Many expressions of the enhancement factor E use the parameter E_∞, which is the enhancement factor for an infinitely fast reaction. In the film theory, it is defined as:

Table 2.3: Different expression for the enhancement factor

Enhancement factor	Reaction type	Reference
$E = \dfrac{\sqrt{Ha^2 \cdot \dfrac{E_\infty - E}{E_\infty - 1}}}{\tanh \sqrt{Ha^2 \cdot \dfrac{E_\infty - E}{E_\infty - 1}}}$	Second-order irreversible reaction	Van Krevelen and Hoftijzer, 1948
$E = \sqrt{\dfrac{4E_\infty(E_\infty - 1)}{1 + Ha^2} \cdot \dfrac{1 + Ha^2}{2(E_\infty - 1)}}$	Second-order irreversible reaction	Astarita et al., 1983
$E = Ha$	Pseudo-first order reaction	Kucka et al., 2003

$$E_\infty = 1 + \frac{D_{MDEA}[R_3N]_B}{2 D_{CO2,L}[CO_2]_i} \qquad (2.82)$$

- D_{MDEA} is the diffusion coefficient of MDEA in water (m²/s)
- $D_{CO2,L}$ is the diffusion coefficient of CO2 in the liquid phase (m²/s)

2.5 Absorption of gases in packed column

Packed bed absorbers are the most common absorbers used for gas removal. Packed columns disperse the scrubbing liquid over packing material, which provides a large surface area for gas-liquid contact.
Packed beds are classified according to the relative direction of gas-to-liquid flow.

- Types of Packed Bed Absorbers

The most common packed bed absorber is the counter-current flow tower shown in Figure 2.6. The gas stream being treated enters the bottom of the tower and flows upward through the bed of packing material.

Liquid is introduced at the top of the packed bed by sprays or weirs and flows downward over the packing material, resulting in the highest theoretically

achievable efficiency. The most dilute gas is put into contact with the least saturated absorbing liquor. Accordingly, the maximum concentration , difference between the gas phase contaminants and the dissolved concentration of the contaminant in the liquid is at the top of the packed bed. This concentration difference provides a driving force for continued absorption.
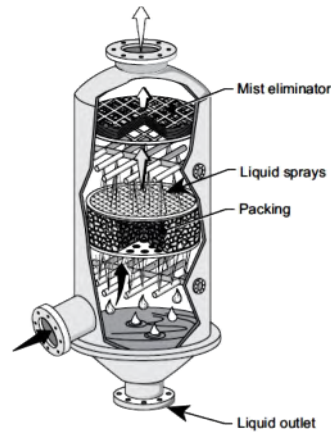
Figure 2.5: Counter-current packed tower

In a cross-flow absorber, the gas stream flows horizontally through the packed bed, which is irrigated by the scrubbing liquid flowing down through the packing material. A typical cross-flow absorber is shown in Figure 2.7 . Inlet sprays aimed at the face of the bed (not shown in Figure 2.7) may also be included.

The leading face of the packed bed is often slanted in the direction of the in-coming gas stream as shown in Figure 2.7. This ensures complete wetting of the packing by allowing the liquid at the front face of the packing enough time to drop to the bottom before being pushed back by the entering gas.
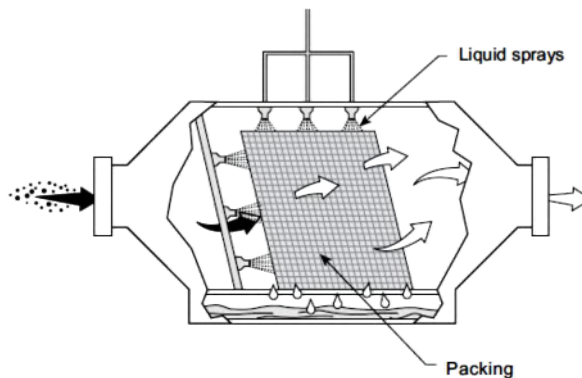
Figure 2.6: Flowchart of cross-flow scrubber

Cross-flow absorbers require complex design procedures because concentration gradients exist in two directions in the liquid: from top to bottom and from front to rear.

Packed bed absorbers are most suited to applications where high gas removal efficiency is required, and the exhaust stream is relatively free from particulate matter. In the production of both sulfuric and hydrochloric acids, packed bed absorbers are used to control tail and exhaust emissions (i.e., SO2 and HCl respectively). The scrubbing liquor for these processes can be a weak acid solution with the spent liquor from the packed tower sent back to the process. Packed towers are also used to control HCl and H_2SO_4 fume emissions from pickling operations in the primary metals industry. They are used to control odors in rendering plants, petroleum refineries, and sewage treatment plants. For odor control applications, the packed bed scrubbing liquor usually contains an oxidizing reagent such as sodium hypochlorite. In these applications, an acid backwash must be added if a precipitate is formed or if plugging can be a problem.The gas flow rate through packed towers can vary from 5 to 30,000 ACFM (0.14 to 850 m3/min).

The packing material provides a large surface area for mass transfer. These packing are usually made of plastic (polyethylene, polypropylene, or polyvinylchloride), but can be ceramic or metal. A specific packing is described by its trade name and overall size. The overall dimensions of packing materials normally range from 1 to 4 inches (2.5- to 10.1-centimeter).

Packing material may be arranged in an absorber in either of two ways. The packing may be dumped into the column randomly or stacked as structured material. Randomly packed towers provide a higher surface area (ft2/ft3), but also cause a higher pressure drop than stacked packing. In addition to the lower pressure drop, the stacked packing provides better liquid distribution over the entire surface of the packing.

- Liquid Distribution.

One of the requirements for efficient absorption is good gas-liquid contact throughout the entire packed bed. The performance of the liquid distributors in the absorber is important to achieve good gas-liquid contact. Liquid should be distributed over the entire upper surface of the packed bed. This is commonly achieved by weirs or feed tube arrangements as shown in Figure 5-8. Arrays of spray nozzles are also used. However, distributors similar to the units are more flexible with respect to variations in the liquid recirculation rate.

(a) Riser orifice   (b) Notched riser

(c) Trough and weir type   (d) Perforated pipe
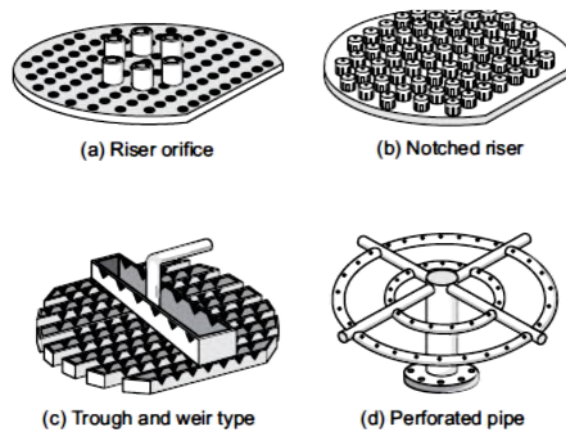
Figure 2.7: Types of liquid distributors for packed bed absorbers

Once the liquid is distributed over the packing, it flows down by the force of gravity through the packing, following the path of least resistance. The liquid tends to flow toward the tower wall where the void spaces are greater than in the center. Once the liquid hits the wall, it flows straight down the tower(channels). It is necessary to redirect the liquid from the tower wall back to the center of the column. Liquid redistributors are used to funnel the liquid back over the entire surface of packing. Redistributors are usually placed at intervals of no more than 10 feet (3.1 meters), or 5 tower diameters, whichever is smaller.1 Uniform distribution of the inlet gas stream is also very important for achieving good gas-liquid contact. This is accomplished by properly designing the inlet gas ducts and the support trays that hold the packing material.

2.6 Previous work

- *Modeling*

Pacheco and Rochelle (1998) Developed a general frame work that can be used to model the interfacial heat and mass transport processes that take place during reactive absorption when both rate and equilibrium controlled reactions take place in the liquid phase.

Mandala et al (2001) Investigate CO_2 absorption into aqueous blends of methyldiethanolamine (MDEA) and monoethanolamine (MEA), as well as 2-amino-2-methyl-1-propanol (AMP) and monoethanolamine (MEA). The combined mass transfer–reaction kinetics–equilibrium model to describe CO_2 absorption into the amine blends has been developed according to Higbie's penetration theory following the work of Hagewiesche et al. (Chem. Eng. Sci. 50 (1995) 1071).

Bolhàr-Nordenkampf et al (2004) implement a rate-based algorithm in Aspen (RATEFRACTM) to yield a predictive tool for MDEA acid gases scrubbing processes. And a new enhancement model is developed to account for the chemical reactions in the liquid phase. New correlations for geometric data, like hold-up and interfacial area, and for reaction rates are provided to give reliable results.

Qian et al (2009) obtained analytical expression of the concentration distribution of CO_2 as a function of time and penetration depth in liquid film, and that of the gas-liquid mass transfer coefficient in RPB Based on Higbie's penetration theory. A mathematical model is developed in this work to quantitatively describe the gas-liquid mass transfer process with reversible reactions in a RPB.

Mudhasakul et al (2013) Study a mixed solvent composed of MDEA and piperazine, called a-MDEA, was. In the first part of this study, an Aspen Plus simulation model of an existing commercial CO_2 capture process called the Acid Gas Removal Unit using a-MDEA was developed in order to validate its accuracy against plant design data and actual data. In the second part of the study, the

validated simulation model in the first part was used to carry out sensitivity analyses.

Yusuff et al (2014) develop a mathematical model able to represent both mass transfer and chemical reaction processes at a given operating conditions for the reactive absorption of CO_2 in an absorption tower and solved it analytically by Matrix method via Excel.

- *Kinetics*

Haimour and Sandall (1984) Measured CO_2 Gas absorption rates in methyldiethanolamine (MDEA) solutions using laminar liquid jet. They found that for the short contact times of these absorption experiments there is only a small effect of any reaction between carbon dioxide and MDEA. Their work represents an experimental confirmation of the N_2O/CO_2 analogy used to estimate the solubility and diffusivity for CO_2 in aqueous MDEA solutions.

Versteeg And Swaaij (1987) Study the reaction between CO_2 and tertiary alkanolamines (MDEA, DMMEA, TREA) in aqueous solutions at various temperatures. Also the absorption of CO_2 in a solution of MDEA in ethanol has been studied

Swaaij And Versteeg (1990) Study the reaction of CO_2 with TEA, DMMEA, and DEMEA at 293, 303, 318 and 333 K. They argued that the contribution of the CO_2 reaction with OH- to the observed reaction rate may have been overestimated in most literature on tertiary amine kinetics as serious depletion of OH- toward the gas-liquid interface usually occurs.

Little et al (1991) have Study the kinetics of the reaction of CO_2 with various alkanolamines (MEA, DGA, DIPA, DEA, and MMEA) in aqueous solutions as a function of temperature. Also kinetic data at 303 K were obtained for the reaction between CO_2 and the cyclic amine morpholine in aqueous solutions

Aliabad and Mirzaei (2009) have presented a theoretical investigation of the simultaneous absorption of CO_2 and H2S into aqueous solutions of MDEA and DEA.

Samanta and Bandyopadhyay (2010) Study experimentally and theoretically the absorption of CO_2 into aqueous solutions of mixtures of small amounts of fast reacting PZ and much larger amounts of MDEA

Ahmady et al (2011) measured The absorption of carbon dioxide in the 4 mol/L aqueous solution of methyldiethanolamine (MDEA) mixed with three types of ionic liquids, 1-butyl-3-methyl-imidazolium tetrafluoroborate ([bmim][BF4]), 1-butyl-3-methyl-imidazolium acetate ([bmim][Ac]) and 1-butyl-3-methyl-imidazolium dicyanamide ([bmim][DCA]) as a function of temperature, CO_2 partial pressure and concentration of ionic liquids in the solution..

Kierzkowska-Pawlak et al (2011) have Study the kinetics of the reaction between CO_2 and methyldiethanolamine in aqueous solutions using the stopped-flow technique at 288, 293, 298 and 303 K. The amine concentration ranged from 250 to 875 mol•m-3.

Huang et al (2011) determined the rate at which CO_2 is absorbed in the solvent system 2-amino-2-methyl-l-propanol (AMP) + Methyldiethanolamine (MDEA) + H2O at 30, 35, and 40 C in a wetted-wall column. Ten different concentrations of the solvent system were used in which MDEA concentration was varied as 1.0 and 1.5 kmol m3; that of AMP, as 0.1, 0.2, 0.3, 0.4, and 0.5 kmol m3. The overall pseudo-first order reaction rate constants for the CO_2 absorption estimated from the kinetics data are presented.

Kierzkowska-Pawlak1and Chacuk1 (2012) have measured the CO_2 absorption rate in aqueous methyldiethanolamine solutions using a stirred cell with a flat gas-liquid interface. The measurements were performed in the temperature range of (293.15 to 333.15) K and amine concentration range of (10 to 20) mass %. Measurements were based on a batch isothermal absorption of the gas. The kinetic experiments were conducted under pseudo-first-order regime. The calculated initial absorption rates enabled to estimate the forward, second order reaction rate constant of CO_2 reaction with MDEA in aqueous solution

[This page is deliberately left blank]

CHAPTER 3

RESEARCH METHODOLOGY

This research was carried out to create a model to simulate CO_2 gas absorption with MDEA in packed bed in non isothermal conditions using rate-based modeling approach and film theory. The simulation results can be used to design the absorber and in optimization of absorber unit operation.

To obtain results in accordance with the purpose of research, it adopted the following methodology:

3.1 Research steps

Study was carried out according to the following stages:

- Study Literature and the previous work which has been done about this subject
- Developing mathematical models with rate-based approach for gas absorption in packed bed by using the concept of enhancement factor
- Numerical solution of developed equations
- Making a program using Matlab program.
- Validation of the developed model against actual plant data.
- The simulation studies were performed to investigate the effect of changing various process variables such as the absorbent concentration, temperature and pressure on the Gas and liquid components Distribution results and recovery percent.

3.2 Mathematical Model Development

On the development of a mathematical model of the absorption of CO_2 from flue gas to a solution of MDEA with packed bed required knowledge about chemical reaction systems, reaction kinetics and mass balance.

3.2.1 Chemical reaction system / Reaction kinetics data

- Chemical Reaction System

In the reaction of tertiary amines with CO_2, a protonated amine and bicarbonate ions are produced. The reaction is consistent with a single step mechanism and water must be present for this reaction to proceed. According to Donaldson and Nguyen (Donaldson and Nguyen, 1980), the reaction can be described as a base catalyzed hydration of CO_2:

$$CO_2 + R_3N + H_2O \xrightleftharpoons{k_2, K_1} R_3NH^+ + HCO_3^- \qquad (3.1)$$

The following reactions also occur in aqueous solutions:

$$CO_2 + OH^- \xrightleftharpoons{k_{OH}, K_2} HCO_3^- \qquad (3.2)$$
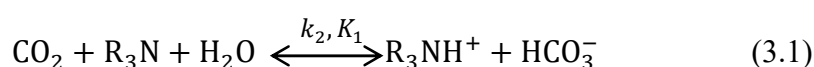
Reactions (3.1)-(3.2) take place in parallel with the finite rates which are described by the forward second order rate constants k_2 and k_{OH} and equilibrium constants K_1 and K_2

In the present work, the simplified kinetic model was applied which assumes that the main reaction (3.1) of CO_2 with MDEA is reversible and the contribution of reaction (3.2) on the mass transfer rate is negligible.

k_2 will be calculated using the correlation obtained in the work Kierzkowska pawlak er al, 2011

$$k_2 = 1.78 \times 10^{10} \exp(\frac{-6441.9}{T}) \qquad (3.3)$$

The other reaction that takes place in the process is the absorption of CO_2 by potassium glycinate the reaction is

$$CO_2 + 2OO - R - NH_2^- \xrightleftharpoons{k_6} OOC - R - NH - COO^- + -OOC - R - NH_3^+ \qquad (3.4)$$
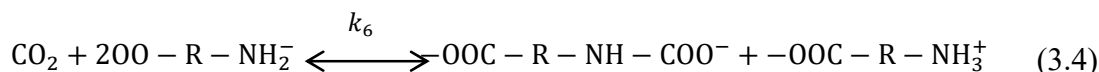
k_6 is the forward reaction constant which is given by the correlation obatained in the work of Portugal et al (2007)

$$k_6 = 2.81 \times 10^{10} \exp(\frac{-5800}{T}) \qquad (3.5)$$

The conditions for the absorption of CO_2 in MDEA and glyk solutions were selected in such a way as to ensure that the absorption occurs in the fast pseudo-first order reaction regime. After these assumptions, the total rate of CO_2 reaction in an aqueous solution of MDEA may be expressed as:

$$r_{ov} = \{k_2[MDEA]_B + k_6[Glyk]_B\}([CO_2] - [CO_2]_e) \qquad (3.6)$$

The overall reaction kinetic constant kov is defined as:

$$k_{ov} = k_2[MDEA]_B + k_6[Glyk]_B \qquad (3.7)$$

$$C_{CO2,e} = \frac{K_3[HCO_3^-]^2}{K_2[CO_3^{-2}]} \qquad (3.8)$$

- $[MDEA]_B$ is the MDEA concentration in the solution.

- $[Glyk]_B$ is the potassium glycinate concentration in the solution.

3.2.2. Mathematical models of Absorption Process

- Reactive absorption

Main method to include chemical reactions in the rate-based mass transfer models are described

$$N_A = k_l a([A]_i - [A]_e)E \qquad (3.9)$$

- N_A is the mass transfer of component i (kmol/s)
- k_L is the overall mass transfer coefficient (m/s)
- a   is the interface area (m²)
- $[A]_i$ is the concentration of component A at the interface
- $[A]_e$ is the equilibrium concentration of component A in the bulk (kmol/m³)
- E   is the enhancement factor (-)

Kucka et al,2003 showed that in the case of pseudo first order reaction, the enhancement factor reduced to Hatta number defined as:

$$Ha = \frac{\sqrt{D_{AL}k_{ov}}}{k_L^0} \tag{3.10}$$

- D_{AL} is the diffusion coefficient of component A in the liquid phase (m²/s)
- k_{ov} is the overall kinetic constant of the chemical reaction (m³/mol.s)
- k_L^0 is the physical mass transfer coefficient (m/s)

3.2.3 Mass and Heat Transfer Coefficient

Gas side mass transfer coefficient is obtained from the empirical correlation by Onda et al (1982). shown in Equation 3.29 where constant A equal to 2 for packing diameter less than 0.012 m and equal to 5.23 for packing diameter greater than 0.012 m.

$$k_G = \frac{A}{RT} (R_{eG})^{0.7} (S_{cG})^{1/3} (ad_p)^{-2.0} (aD_{kG}) \tag{3.11}$$

Reynold and Schmidt number are defined as, respectively:

$$R_{eG} = \frac{G}{a\mu_g} \qquad S_{cG} = \frac{\mu_g}{\rho_g D_{kM}} \tag{3.12}$$

Liquid side mass transfer coefficient is obtained from the empirical correlation by Taylor and Krishna (1993) shown in Equation 3.30:

$$k_{L,k} = 0.0051 \, (R_{eL})^{2/3} (S_{cL})^{-0.5} (a_p d_p)^{0.4} (\frac{\mu_L g}{\rho_L})^{1/3} \tag{3.13}$$

Reynold and Schmidt number are defined as, respectively:

$$R_{el} = \frac{L}{a\mu_L} \qquad S_{cL} = \frac{\mu_L}{\rho_L D_{AL}} \tag{3.14}$$

Gas-liquid interfacial area per unit volume of packed column, a, is obtained from packing specific area from the correlation provided by Onda et al (1982).

$$\frac{a}{a_p} = 1 - \exp[-1.45(\frac{\sigma_c}{\sigma_L})^{0.75} (R_{eL})^{0.1} (F_{rL})^{-0.05} (W_{eL})^{0.2} \tag{3.15}$$

In Equation 3.32, Froude and Weber number are defined as, respectively:

$$F_{r,L} = \frac{a_p L^2}{\rho_L^2 g} \qquad W_{e,L} = \frac{L^2}{\rho_L a_p \sigma} \qquad (3.16)$$

Diffusion coefficient of species in gas phases was determined from binary diffusion coefficient using Maxwell-Stevan equation as follows:

$$\frac{1}{D_{im}} = \frac{\sum(\frac{1}{D_{ij}})(x_j N_i - x_i N_j)}{N_i - x_i \sum N_j} \qquad (3.17)$$

Where the binary diffusion coefficient was obtained from correlation by Fuller et al. recommended by Taylor and Krishna (1993) , Reid et al (1987) , and also Daubert and Danner (1985)

$$D_{ij,G} = \frac{1 \times 10^{-7} T^{1.75} (\frac{1}{M_i} - \frac{1}{M_j})}{p(v_i^{1/3} + v_j^{1/3})^2} \qquad (3.18)$$

Due to dilute solution condition, diffusion coefficient of species in liquid phase was assumed binary with respect to water and determined using Wilke and Chang Equation

$$D_{iw,L} = \frac{7.4 \times 10^{-8} T(\emptyset M_w)^{0.5}}{\mu_L v_i^{0.6}} \qquad (3.19)$$

Heat transfer coefficient in gas phase was determined from mass transfer coefficient in gas phase using Chilton-Colburn analogy; the complete Chilton-Colburn analogy is found in Eqs (3.20)

$$\frac{\overline{h_G}}{\rho_G C_{pG}} P_{rG}^{2/3} = k_G S_{CG}^{2/3} \qquad (3.20)$$

While heat transfer resistance in the liquid phase was neglected.

3.2.4 Gas Solubilities

The solubility of gases in promoted MDEA solutions were estimated using modified Henry law with empirical model of Schumpe which describes the solubility of gases in mixed electrolytes solutions considering salting out effects:

$$\log\left(\frac{H_{e,jw}}{H_{e,j}}\right) = \sum(h_i + h_G)c_{i,L} \qquad (3.21)$$

Where h_i is the ion-specific parameter (m^3/kmole), h_G is the gas specific parameter (m^3/kmole) and c_{iL} is the concentration of ion i (kmole/m^3). The Henry constant of gas-water system (can be obtained from Equation (3.22):

$$1/H_{e,jw}(T) = 1/H_{e,jw}(298\ K) * \exp\left(\frac{-d\ln k_H}{d(\frac{1}{T})} * \left(\frac{1}{T} - \frac{1}{298}\right)\right) \qquad (3.22)$$

The value of $H_{e,jw}$ (298 K) and -d ln k_H /d(1/T) are shown in Table (3.1)

Table 3.1 The values of $H_{e,jw}$(298 K) and $\dfrac{-d\ln k_H}{d(\frac{1}{T})}$ for various gases

Component	$1/H_{e°298\ K}$ (kmol/m^3. Pa)	- dln k_H/d($\frac{1}{T}$)
CO_2	7.57×10^{-7}	2200
N_2	6.02×10^{-9}	1300
CH_4	1.38×10^{-8}	1600

Gas specific parameter was extended from Equation (3.21) to wider temperature range using Weissenberger and Schumpe method and expressed in Equation (3.23).

$$h_G = h_{C,0} + h_T\ (T - 298.15) \qquad (3.23)$$

Table 3.2 The value of gas parameter

Component	$h_{G,0}$ (m^3/kmole)	h_T (m^3/kmole. K)
CO_2	-1.72×10^{-5}	-3.38×10^{-7}
N_2	-1×10^{-6}	-6.05×10^{-7}
CH_4	2.2×10^{-6}	-5.24×10^{-7}

In equation (3.23), h_T is the temperature correction (m^3/kmole.K). The values of h_{i+}, h_{i-}, $h_{G,0}$, and h_T can be seen in Table (3.2) and Table (3.3) .Equations (3.23) and (3.22) are substituted into Equation (3.21) to obtain the value of $H_{e,j}$.

Table 3.3 The value of ion specific parameter

Cation	h_i^+ (m^3/kmole)	Anion	h_i^- (m^3/kmole)
K^+	0.0922	HCO_3^-	0.0967
$MDEAH^+$	0.041	CO_3^{2-}	0.1423
H^+	0	OH^-	0.0610
		Gly^-	0.0413

3.2.5 Mathematical models of Absorption Process in packed Column

This study was conducted with the theoretical approach (simulation) by developing mathematical model for heat and mass transfer phenomena accompanied by chemical reaction in CO_2 removal process at non-isothermal condition using MDEA aqueous solution (Altway A et al ,2015).

The model is based on the following assumptions:

• Steady state and adiabatic operations

• Plug-flow pattern for gas and liquid

• Neglected amount of solvent evaporation and

• Constant pressure throughout the column.

• The reaction in the liquid phase is fast enough for a substantial amount of the gas absorbed to react in the liquid film, rather than to be transferred unreacted to the bulk.

Mathematical model development was conducted by constructing differential mass and energy balances in the packed column. Figure (3.1) shows schematic diagram of packed bed absorption column showing an infinitesimal element for mass and energy balances. Microscopic or differential mass and energy balance was constructed based on System I, while macroscopic balance to correlate several process variables in packed column was constructed through System II (see Figure 3.1).
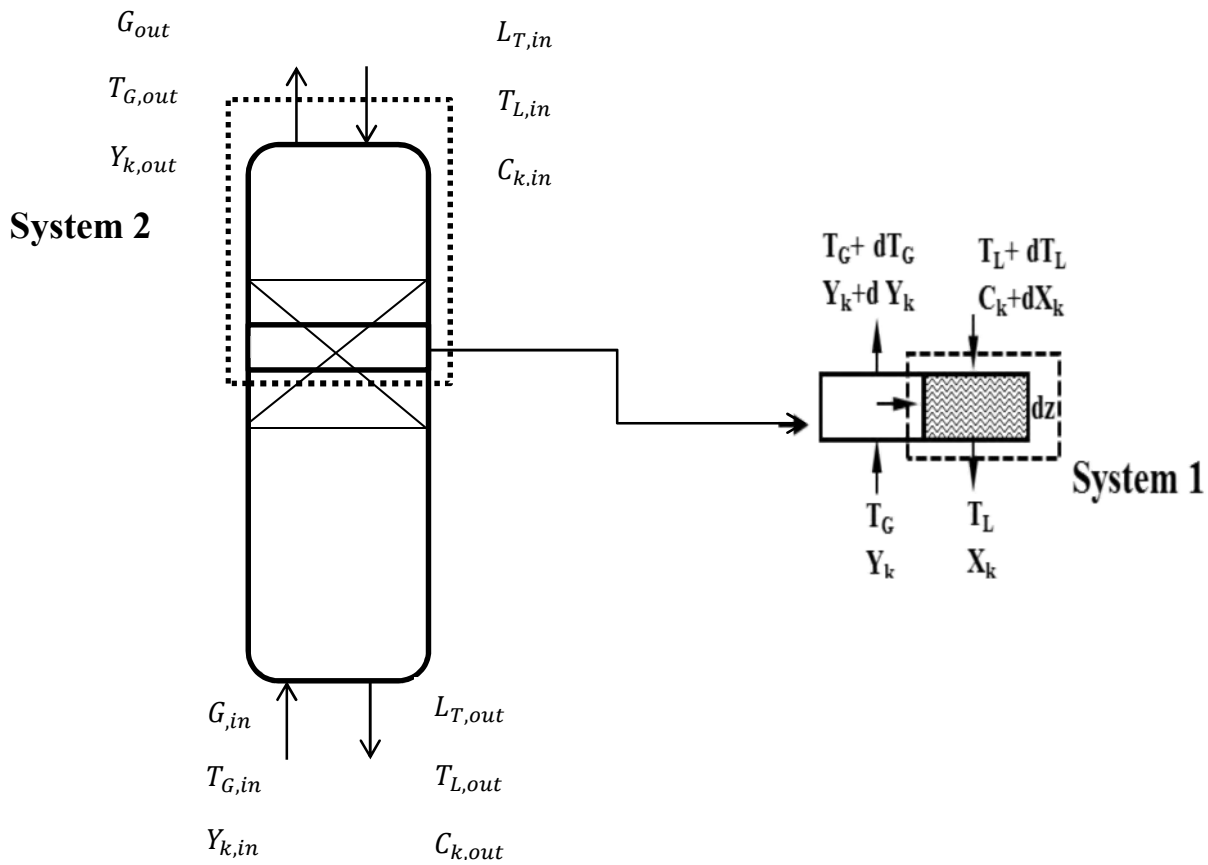
Figure 3.1: Schematic diagram of packed bed absorption column showing an infinitesimal element for mass and energy balances

Differential Mass Balances:

The parameter used:

A: Sectional area of the column, m^2

a: Gas-liquid interfacial area per unit volume of packed column, $m^2 \cdot m^{-3}$

C: Molar density, $kmole \cdot m^{-3}$

$[A]_i$: Concentration of component A at interface, $kmole \cdot m^{-3}$

$[A]_e$: Equilibrium concentration of A in liquid phase, $kmole \cdot m^{-3}$

$[A]_B$: Bulk concentration of A in liquid phase, $kmole \cdot m^{-3}$

G: Mass velocity of gas, $kg \cdot m^{-2} \cdot s^{-1}$

L_{in} : Inlet molar flow rate of liquid, $kmole \cdot s^{-1}$

M_i : Molecular weight of component i, $kg \cdot kmole^{-1}$

N_{CO2} : Molar flux (absorption flux) of CO2, kmole.m^{-2}s^{-1}

x_i : Mole fraction of component i in liquid phase

X_i : Molar ratio of component i (mole component i per mole inlet liquid)

y_i : Mole fraction of component i in gas phase

Y_i : Molar ratio of component i (mole component i per mole inlet gas)

Z_T : Height of packing ,m

L : Liquid hold up in packed column

r_{CO2} : Reaction rate of CO_2, kmole. m^{-3}s^{-1}

System I

Conservation law   : In - Out+ Rate of Reaction=Accumulation

- CO2:

$$N_{CO2}aAdz + L_{in}dX_{CO2} = r_{CO2}\phi_L Adz$$

$$L_{in}dX_{CO2} \cong 0$$

$$N_{CO2}aAdz = r_{CO2}\phi_L Adz \tag{3.24}$$

- MDEA

$$-L_{in}dX_{MDEA} - r_{CO2}\emptyset_L Adz = 0 \tag{3.25}$$

- k (dissolved gas):

$$L_{in}dX_k - N_k aAdz = 0 \tag{3.26}$$

Equation 3.24 was substituted to Equation 3.25 to yield

$$-L_{in}dX_{MDEA} - N_{CO2}a\,Adz = 0 \tag{3.27}$$

$$\frac{dX_{MDEA}}{dz} = -\frac{N_{CO2}aA}{L_{in}} \tag{3.28}$$

When $N_{CO2}a$ was substituted from then the following equation was obtained after some rearrangements

$$\frac{dX_{MDEA}}{d\zeta} = -\frac{Ek_{L,CO2}aC(x^*_{CO2}-x^e_{CO2})Z_TA}{L_{in}} \qquad (3.29)$$

Where $\zeta=Z/Z_T$ and $x_{MDEA} = [MDEA]_B/C$

For k (dissolved gas)

$$\frac{dX_k}{dz} = \frac{N_kaA}{L_{in}} \qquad (3.30)$$

Where N_ka was obtained from $N_ka = k_{L,k}a([k]_i - [k]_B)$, and Equation (3.30) can be rearranged as follows

$$\frac{dX_k}{d\zeta} = \frac{k_{L,k}aC(x^*_k-x^0_k)Z_TA}{L_{in}} \qquad (3.31)$$

The concentration of bicarbonate ion was deter-mined using stoichiometry as follows:

$$X_{HCO_3^-} - X_{HCO_{3,in}^-} = X_{MDEA,in} - X_{MDEA} \qquad (3.32)$$

The concentration of other species (expressed as mole ratio) in liquid phase was determined using equilibrium and electro neutrality constrain. Molar concentration of various species in liquid phase was determined from $[i] = x_i . C$, where mole-fraction, x_i, was determined from mole ratio as follows:

$$x_i = \frac{X_i}{\sum X_k} y_i = \frac{Y_i}{\sum Y_k} \qquad (3.33)$$

And molar density, C, was calculated from liquid mass density as $C = \rho_L/M$, where M is molecular weight of liquid mixture, $M=\sum M_I x_i$, and ρ is its density.

The presence of catalyst in the liquid phase does not affect significantly liquid density.

The concentration of CO_2 and carrying gases in the gas phase can be obtained by performing a mass balance over System II:

CO_2:

$$G_{m,in}[Y_{CO2} - Y_{CO2,out}] = L_{min}[X_{MDEA,in} - X_{MDEA}] \qquad (3.34)$$

k (carrying gases):

$$G_{m,in}[Y_k - Y_{k,out}] = L_{min}[X_{k,in} - X_k] \qquad (3.35)$$

CO_2 concentration on the interface (C^*_{CO2}):

$$[CO_2]_i = \frac{k_{G,CO2} y_{CO2} \, P + E \, k_{L,co2}[CO_2]_e}{E k_{L,CO2} + k_{G,CO2} \, H_{CO2}} \tag{3.36}$$

Concentration of other gases on the interface (C_k^*):

$$[k]_i = \frac{k_{G,k} y_k \, P + E \, k_{L,k}[k]_e}{E k_{L,k} + k_{G,k} \, H_k} \tag{3.37}$$

Differential heat balance on the gas side is given in Equation (3.38):

$$\frac{dT_G}{dz} = \frac{h_G a}{C_{pG} G}(T_G - T_L) \tag{3.38}$$

While liquid temperature was calculated from energy balance for System II:

$$T_L = T_{L,in} + \frac{G C_{pG}}{C_{pL}}\left[C_{pG}(T_G - T_{G,in})\right] - (-\Delta H_{rx})\frac{G_{in}}{L C_{pL}}\left[Y_{CO2,in} - Y_{CO2}\right] \tag{3.39}$$

3.3 Numerical solution Equations (3.29) and (3.31) were solved numerically using orthogonal collocation method with 6 internal collocation points, thus

$$X_{MDEA,j} = X_{MDEA,in} - \frac{v_B Z_T}{H_{T,CO2}} \sum_{i=0}^{NC+1} H_{ji} E_i \left(x_{CO2,i} - x_{CO2,e}\right) \tag{3.40}$$

$$X_{kj} = X_{kin} + \frac{Z_T}{H_{T,k}} \sum_{i=0}^{NC+1} H_{ji}\left(x_{k,i} - x_{k,B}\right) \tag{3.41}$$

$$T_L = T_{L,out} + \frac{G C_{pG}}{L C_{pL}}\left[(T_G - T_{G,in})\right] - (-\Delta H_{rx})\frac{G_{in}}{L C_{pL}}\left[Y_{CO2,in} - Y_{CO2}\right]$$

$$\tag{3.42}$$

$$T_{G,j} = T_{G,out} - N_G \sum_{m=1}^{NC+2} H_{jm}\left(T_{G,m} - T_{L,m}\right) \tag{3.43}$$

$$H_{T,CO2} = \frac{L_{in}}{A k_{L,CO2} a C} \;,\quad H_{T,k} = \frac{L_{in}}{A k_{L,k} a C} \;,\quad N_G = \frac{h_G a Z_T}{C_{pG} G} \tag{3.44}$$

$$\text{Removal percentage} = 1 - \frac{Y_{CO2,out}}{Y_{CO2,in}} \tag{3.45}$$

3.4 Making Program Making the computer program of mathematical models that have been developed using Mat lab.

3.5 Validation of the developed Model Validation is done by comparing the results of the simulation predictions with real data of an existing natural gas sweetening process in Thailand called Acid Gas Removal Unit (AGRU), here the real data of the plant:

- Absorber configurations.

Packing of stages	IMTP 50-MM
Section diameter (m)	4.1
Section Packed height(m)	14.1
Column pressure(atm)	41.06

- Feed gas and solvent compositions

  o Inlet gas

Flow rate (kg/h)	336,520
Composition (mol %)	
CO_2	19.31
N_2	1.33
CH_4	79.36
Temperature (°C)	25
Pressure (atm)	41.06

  o Amine solvent

Flow rate(kg/h)	1,016,300
Composition (mol %)	
MDEA	45.00
PZ	5.00
H_2O	50.00
Temperature (°C)	52
Pressure (atm)	41.06

3.6 Develop a simulation model with an amino acid promoter, potassium glycinate, instead of piperazine in the same gas feed condition and column configurations. the influence of various operating conditions such as the potassium glycinate concentration, solvent feed flow rate , feed temperature of both gas and liquid stream, and finally the pressure of the absorber on CO_2 absorptive capability have been examined .

.

CHAPTER 4

RESULTS AND DISSCUSION

This study was carried out by constructing a simulation program for CO_2 gas absorption from flue gas using Methyldiethanolamine solution (MDEA) with Potassium glycinate as promoter at industrial packed column. The research was done by making a simulation model for CO_2 gas absorption with reversible reaction and in non-isothermal conditions. The work consists of two parts. The first part focused on creating a simulation program for the reactive absorption process. Data for thermodynamic properties and chemical reactions used in the simulation were gleaned from previous experimental studies on the MDEA-PZ-CO_2 system. After the program had been done it was validated against plant data of an actual process. Input for unit operating conditions, mass balances, and energy balances in the model were based on actual data of an existing natural gas sweetening process in Thailand called Acid Gas Removal Unit (AGRU).to validated the model. The results of the simulation were compared with the actual data to demonstrate the accuracy of the developed simulation program.

The second part of this study is to develop a simulation model with an amino acid promoter, potassium glycinate, instead of piperazine in the same gas feed condition and column configurations. the influence of various operating conditions such as the potassium glycinate concentration, solvent feed flow rate , feed temperature of both gas and liquid stream, and finally the pressure of the absorber on CO_2 absorptive capability have been examined .

4.1 Model validation

The rate-based process model was validated against the actual data of an existing natural gas sweetening process in Thailand called Acid Gas Removal Unit (AGRU) to remove CO_2 from process gas stream containing 19.31% CO_2, 1.33 % N_2, and 79.36 % CH_4 with flow rate of 336.52 ton/hr. The CO_2 is removed from the gas stream by counter current absorption Column with diameter of 4.1 m. The column is filled with 5 cm IMPT packing .Lean solution, containing 45 %

MDEA and 50 % water , was fed into the top of part column .To enhance the absorption rate, a promoter, Piperazine ,was added into the solution. It can be seen from Table 1 that for the same operating condition the predicted percent CO_2 removal is 95.8679% compared to 99.58% in AGRU removal unit. This may be due to the use of empirical correlations for the estimation of thermodynamic and transport properties and parameters associated with mass transfer in the absorption rate, neglecting the solvent evaporation in the energy balance. And finally due to the assumption that the packed column exhibit a perfectly plug flow behavior where actually there is a little deviations from this ideal behavior.

Although some discrepancies exist in the model, the proposed model is sufficiently accurate to describe the characteristics and performance of the AGRU that uses a-MDEA as the absorptive solvent.

Table 4.1 Comparison between simulation result and actual plant data

Variable comparison	Simulation	AGRU Removal Unit
Flow rate of gas (kg/h)	336,520	336,520
Flow rate of lean solution (kg/h)	1,016,300	1,016,300
Temperature of gas (K)	298	298
Temperature of lean solution (K)	325	325
Pressure (atm)	41.06	41.06
CO_2 removal (%)	95.8679	99.58

4.2 Simulation

The AGRU model proposed in the previous section was used as the base case to study the effect of different promoter (potassium glycinate) in the absorption process efficiency with same condition as it is in the plant. The effluence of different process parameters on the CO_2 recovery has also been examined. The results of the simulation are given below.

4.2.1 Liquid Concentration Distribution in Packed Column

The predicted concentration distribution of MDEA and MDEAH+ in the case of potassium glycinate promoter are shown in Figure 4.1. it show the concentration distribution against axial position (through column height) where 0 represent the top of the column where solvent stream is fed ,and 1 is the bottom of column and the location of output solvent stream. From Figure 4.1, it can be seen that the MDEA mol fraction decreases as liquid moves down the column . Where the initial mol fraction of MDEA is 0.1183 and the outlet MDEA mol fraction is 0.0335. It is because the MDEA solution reacts with CO_2 gas in the packed column forming MDEAH+. Thus, MDEAH+ mol fraction increases from 0.0002 to 0.0850 as the liquid stream flows from the top to the bottom of the column

.
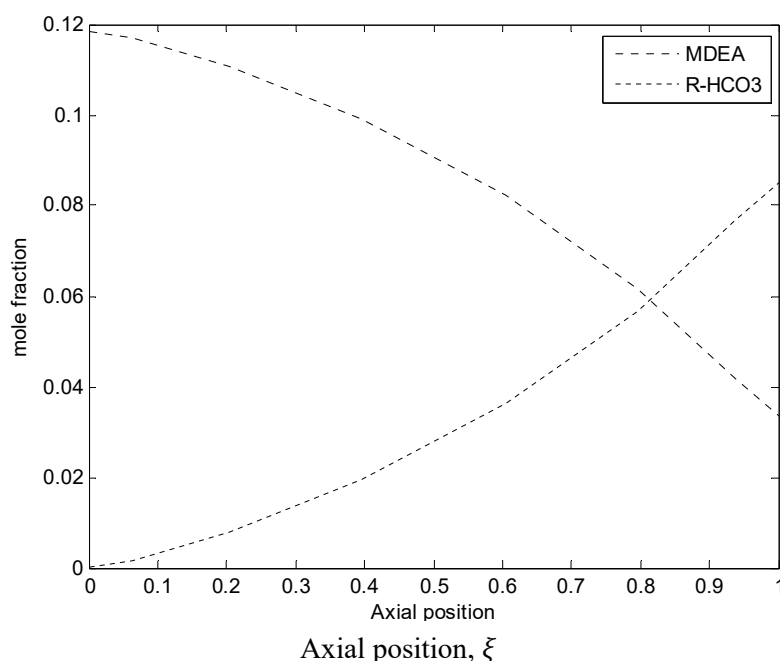
Figure 4. 1:   Concentration distribution of MDEA and MDEAH+ in the column

with Potassium glycinate as promoter

$[T_L : 325 \text{ K} , T_G : 398 \, K , P : 41.06 \, atm \;]$

4.2.2 Gas concentration distribution in the absorber

The direction of flow for gas stream is from the bottom to the top of the column (counter current with the liquid stream) .the concentration distribution of CO_2 with potassium glycinate as a promoter is shown in figure 4.2.it indicates that CO_2 concentration decreases through the height of the column due to the physical and chemical absorption of carbon dioxide by the solvent .the feed mol fraction of carbon dioxide is 0.19 and the exit mole fraction is 0.0195 indicating that 91.6654%. of feed carbon dioxide had been removed.
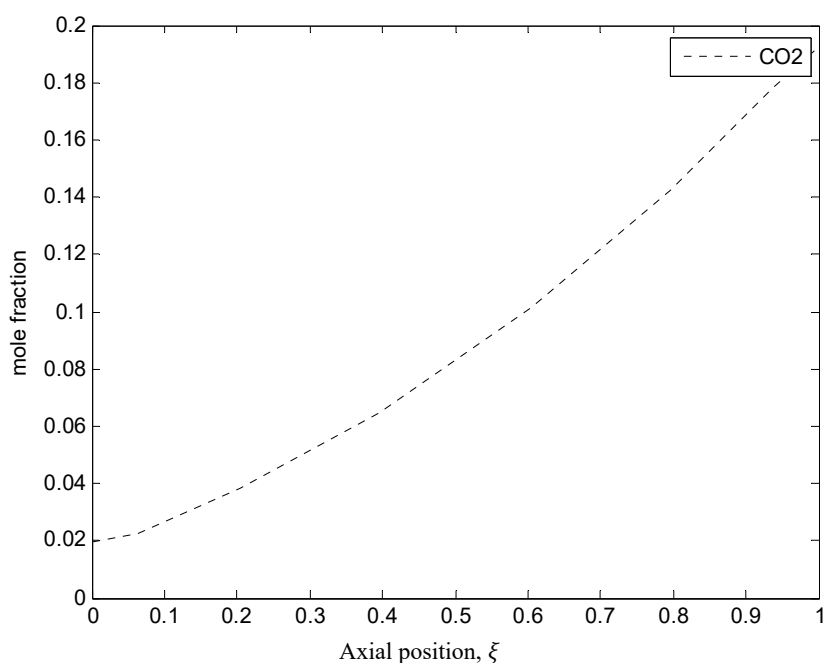
Figure 4. 2: Mole fraction distribution of CO_2 in the gas stream with Potassium glycinate as promoter

$$[T_L : 325 \text{ K} , T_G : 298 \text{ } K, P : 41.06 \text{ } atm]$$

4.2.3 The effect of absorbent flow rate on %CO_2 removal

The effect of absorbent flow rate on % CO_2 removal in the efficiency of the absorption when potassium glycinate is the used as promoter is shown in Figure 4.3 under the operation conditions of 45% MDEA solvent and 5% concentration of potassium glycinate .From Figure 4.3, it can be seen that the

increase of the absorbent flow rate give significant effect on the $\%CO_2$ removal.as it shift the removal of CO_2 From 87.79% when the flow rate is 914,670 kg/hr to 99.008% at flow rate of 1,341,516 kg/hr. It indicates that the liquid side resistance has a considerable effect on the process of CO_2 absorption in MDEA aqueous solution. Although in this simulation the mass transfer resistance of gas side is also counted. The increase of absorbent flow rate will increase the turbulence and driving force and shorten life time of liquid film , consequently the mass transfer coefficient increases so that CO_2 absorption rate increases.
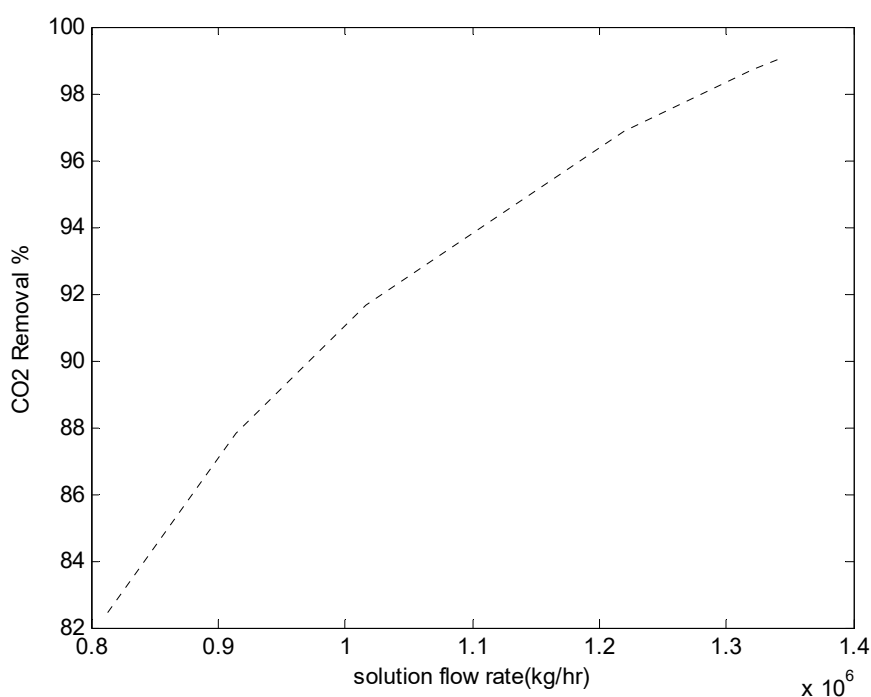
Figure 4.3:   The effect of solution flow rate on %CO2 removal with Potassium
               glycinate as promoter
               $[T_L : 325 \text{ K} , T_G : 298 \text{ K}, P : 41.06 \text{ atm}]$

4.2.4 The Effect of Temperature on $\%CO_2$ Removal

        The effect of lean solution feed temperature on $\%CO_2$ removal with gas stream feed temperature of 298 k and potassium glycinate is the used activator can be seen in Figure 4.4 (a). Figure 4.4 (a) represents that the temperature gives a considerable effect in $\%CO_2$ removal, indicating that the process of absorption of CO_2 into promoted MDEA solution is sensitive to temperature change. A higher

temperature resulting in a higher reaction rate constant according to the Arrhenius equation, a higher diffusivity and a lower gas solubility. The highest CO_2 removal efficiency is 98.89% at lean solution temperature of 365 K. Thus, the increase of absorption rate depends on the relative effect of temperature on the reaction rate constants, diffusivity and solubility of gas absorbed. Hence, it is beneficial for a reactive absorption, to increase temperature to some extent for higher CO_2 removal efficiency.

The effect of gas feed temperature on %CO_2 removal with liquid stream feed temperature of 325 k from simulation result can be seen in Figure 4.4 (b),the higher temperature of gas the high percent of CO_2 will be removed, The highest CO_2 removal efficiency is 98.49% at gas feed temperature of 360 K. Thus, it is beneficial for a reactive absorption, to increase temperature to some extent for higher CO_2 removal efficiency.
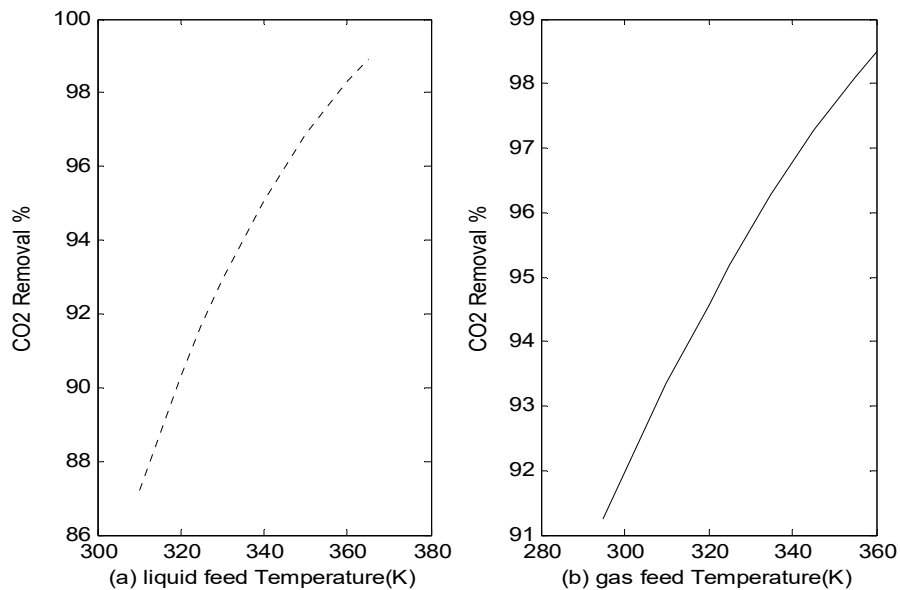
Figure 4. 4:   (a) The effect of solution feed temperature on %CO_2 removal with

Potassium glycinate as promoter

[T_G : 298 K , P : 41.06 atm]

(b) The effect of gas feed temperature on %CO_2 removal with Potassium

glycinate as promoter

[T_L : 325 K , P : 41.06 atm]

4.2.5 The effect of absorber pressure and promoter types on %CO_2Removal

The effect of absorber pressure on %CO_2 removal at liquid feed temperature of 325 K and gas stream feed temperature of 298 K from simulation result can be seen in Figure 4.5. Figure 4.5 shows that CO_2 removal efficiency increases with increasing of operation pressure of the absorption column. This is due to the increasing the pressure will increase gas solubility and therefore the absorption rate. Figure 4.5 show that at pressure of 25 atm, the CO_2 removal efficiency for promoter PZ, and potassium glycinate are 79.2981%; 71.9556%, respectively. Meanwhile, at pressure of 45 atm the CO_2 removal efficiency are 97.8957%; 94.276%, respectively. These show that PZ gives the higher CO_2 removal efficiency compared to potassium glycinate .the main reason behind that is the fast reaction kinetic of PZ compared with potassium glycinate.
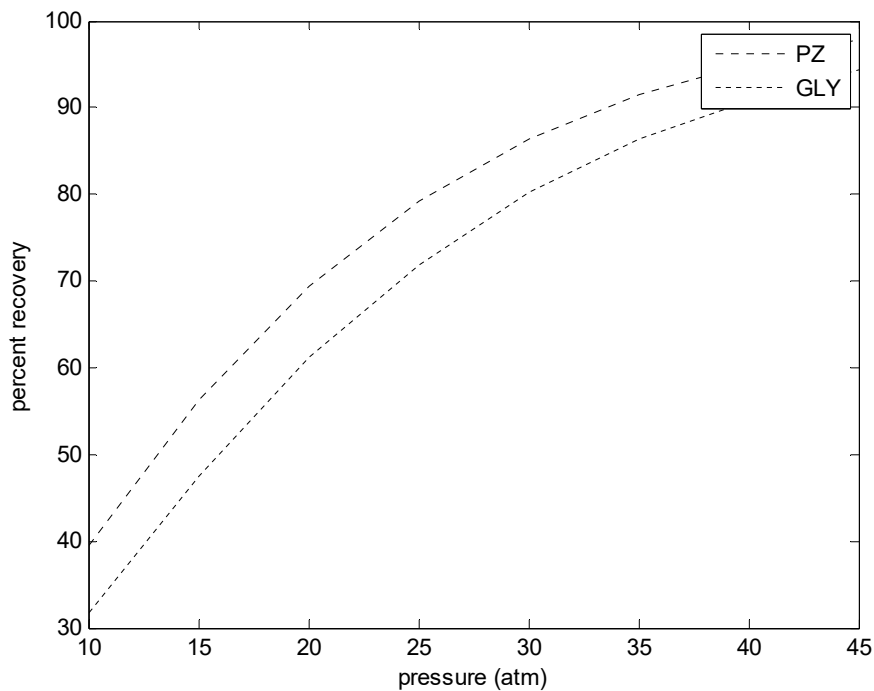
Figure 4.5:   The Effect of Absorber Pressure and Promoter Types on %
              CO_2Removal
              [T_L : 325 K , T_G : 298 K]

4.2.6 The effect of promoter concentration on %CO_2 removal

Figure. 4.6 show the effect of potassium glycinate concentration in the mixed amine solvent on the percent CO_2 recovery in the absorber. It is clear from Fig. 4.6 That the proportion of potassium glycinate in the amine solvent does significantly affect the CO_2 recovery in the absorber. The CO_2 recovery was dramatically enhanced when the potassium glycinate concentration was increased from 0 wt% to 7 wt% but leveled off toward 100% at higher potassium glycinate concentrations. The slope of the curve between 0 wt% and 7 wt% Potassium glycinate was approximately 4. This means that increasing the Potassium glycinate concentration every 1 wt% will enhance the recovery rate by about 4 %. The result also confirmed that the MDEA solvent alone without any activator is not effective in capturing CO_2 since it will leave a large amount of CO_2 in the vented gas.
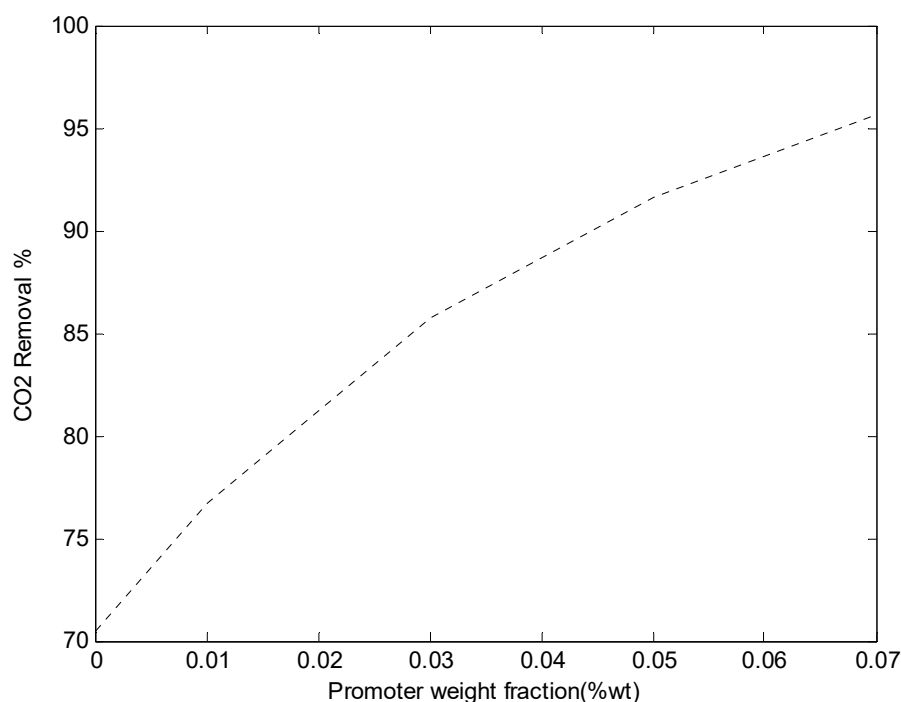
Figure 4.6:   The effect of Promoter weight fraction (Potassium glycinate) on %CO2 removal

$[T_L :\ 325\ \text{K}\ , T_G :\ 298\ K\ , P :\ 41.06\ atm\ ]$

APPENDIX A

MATHEMATICAL MODEL DEVELOPING

```
┌──────────────┐   ┌──────────────┐   ┌──────────────┐
│MASS TRANSFER │   │GASES         │   │REACTIONS     │
│PARAMETERS    │   │SOLUBILITY    │   │KINETICS AND  │
│              │   │              │   │EQUILIBRIUM   │
└──────┬───────┘   └──────┬───────┘   └──────┬───────┘
       │                  │                  │
       └──────────────────┼──────────────────┘
                          │
                ┌─────────▼─────────┐
                │  MATHEMATICAL     │
                │  MODEL DEVELOPING │
                └─────────┬─────────┘
                          │
┌──────────────┐   ┌──────▼───────────┐
│PLANT DATA    │   │PREDICTIONS       │
│              │   │RESULTS           │
└──────┬───────┘   └──────┬───────────┘
       └──────────────────┤
                ┌─────────▼─────────┐
                │VALIDATION AND     │
                │ANALYSIS OF        │
                │DEVELOPED MODEL    │
                └─────────┬─────────┘
                ┌─────────▼─────────┐
                │SIMULATION OF      │
                │INDUSTRIAL         │
                │PACKED COLUMN      │
                └───────────────────┘
```
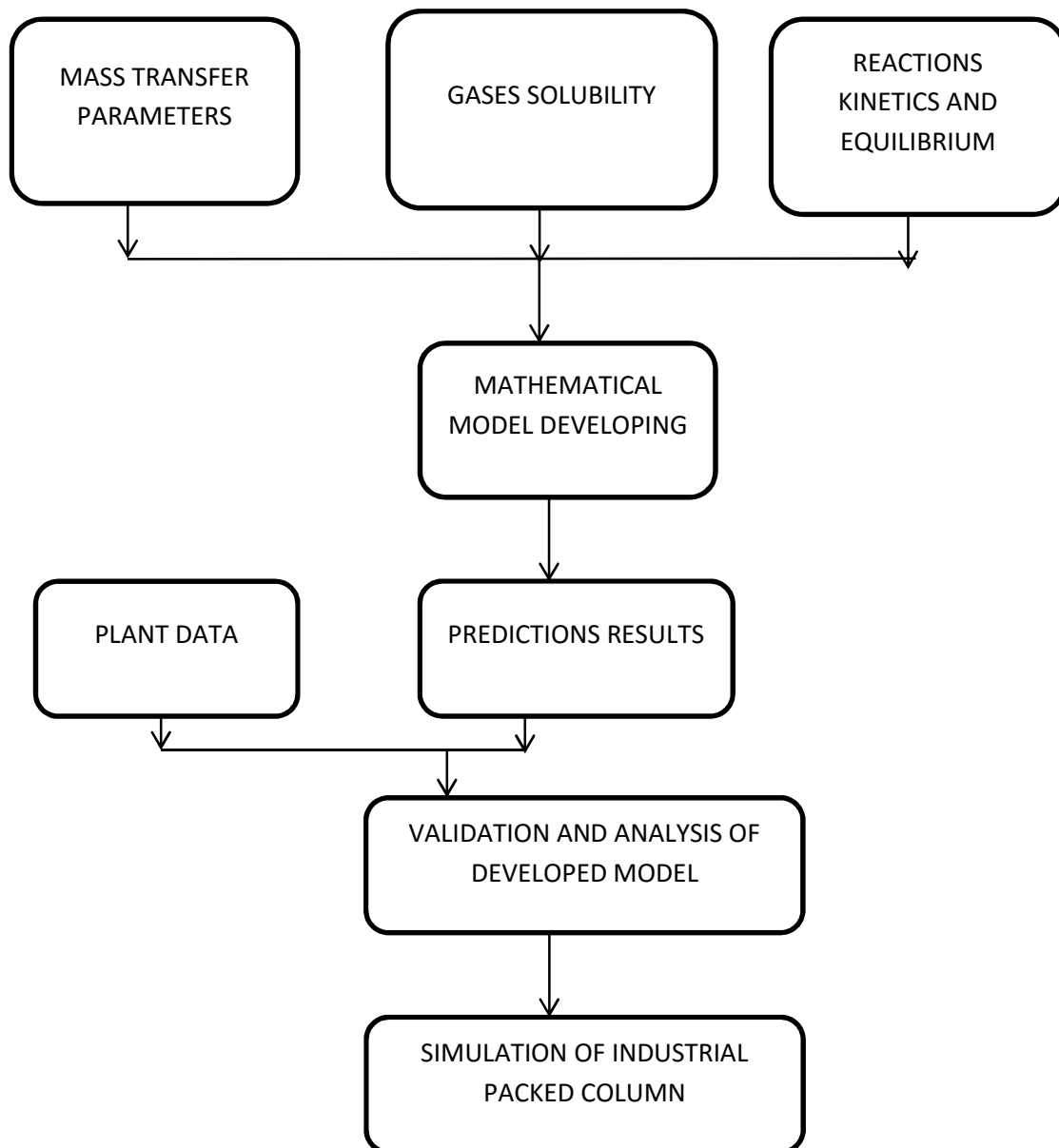
APPENDIX B

NUMERICAL SOLITION EQUATIONS

➢ Reactions Equilibrium Data

Reactions that take place are

$$CO_2 + R_3N + H_2O \xleftrightarrow{k_2, K_l} R_3NH^+ + HCO_3^-$$

$$CO_2(aq) + 2H_2O \leftrightarrow HCO_3^- + H_3O^+$$

$$HCO_3^- + H_2O \leftrightarrow CO_3^{-2} + H_3O^+$$

$$MDEAH^+ + H_2O \leftrightarrow MDEA + H_3O^+$$

$$2H_2O \leftrightarrow H_3O^+ + OH^-$$
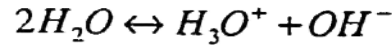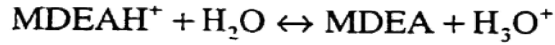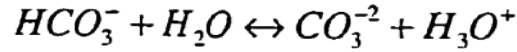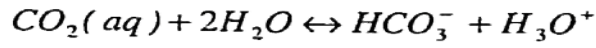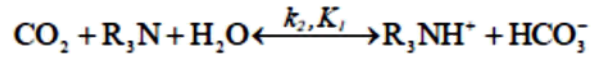
With

$$K_1 = \frac{[R_3NH^+][HCO_3^-]}{[H_2O][R_3N][CO_2]}$$

$$K_2 = \frac{[HCO_3^-][H_3^+O]}{[CO_2][H_2O]^2}$$

$$K_2' = K_2[H_2O] = \frac{[HCO_3^-][H^+]}{[CO_2][H_2O]}$$

$$K_3 = \frac{[CO_3^{-2}][H_3^+O]}{[HCO_3^-][H_2O]}$$

$$K_3' = K_3[H_2O] = \frac{[CO_3^{-2}][H^+]}{[HCO_3^-]}$$

$$K_4 = \frac{[R_3N][H_3^+O]}{[R_3NH^+][H_2O]}$$

$$K_4' = K_4[H_2O] = \frac{[R_3N][H^+]}{[R_3NH^+]}$$

$$K_5 = \frac{[H_3^+O][OH^-]}{[H_2O]^2}$$

$$K_5' = K_5[H_2O] = \frac{[H^+][OH^-]}{[H_2O]}$$

The temperature dependence of the equilibrium constants is expressed as
$$lnK_i = \frac{a_i}{T} + b_i\ lnT + c_i$$

Where ai-ci are constants. Values of these constants for reactions is given in Table below

Parameter	a_i	b_i	c_i	Source
K_2	-12092.1	-36.7816	235.482	Edwards et al,1978
K_3	-12431.7	-35.4819	220.067	Edwards et al,1978
K_4	-4234.98	0	-9.4165	Posey,1996
K_5	-13445.9	-22.4773	140.932	Edwards et al,1978

With

$$K_1 = \frac{K_2}{K_4}$$

$$C_{CO2,e} = \frac{K_3 C_{HCO_3^-}^2}{K_2 C_{CO_3^-}^2}$$

> Reaction kinetics Data

$$CO_2 + R_3N + H_2O \overset{k_2, K_1}{\longleftrightarrow} R_3NH^+ + HCO_3^- \qquad (3.1)$$

$$CO_2 + 2OO - R - NH_2^- \overset{k_6}{\longleftrightarrow} -OOC - R - NH - COO^- + -OOC - R - NH_3^+$$
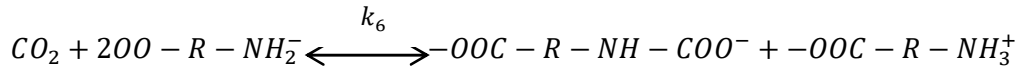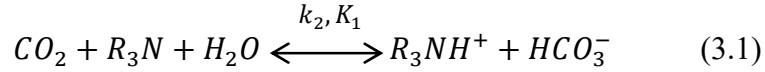
$$r_{ov} = \{k_2[MDEA]_0 + k_6[Glyk]_0\}([CO_2] - [CO_2]_e)$$

$$k_2 = 1.78 \times 10^{10} \exp(\frac{-6441.9}{T})$$

$$k_6 = 2.81 \times 10^{10} \exp(\frac{-5800}{T})$$

> Components Solubility

CO_2 Concentration on the interface (C_{CO2}^*):

$$C_{CO2}^* = \frac{k_{G,CO2} y_{CO2} P + E k_{L,co2} C_{CO2,e}}{E k_{L,CO2} + k_{G,CO2} H_{CO2}}$$

Concentration of other gases on the interface (C_k^*):

$$C_k^* = \frac{k_{G,k} y_k P + E k_{L,k} C_{k,e}}{E k_{L,k} + k_{G,k} H_k}$$

$$\log\left(\frac{H_{e,jw}}{H_{e,j}}\right) = \sum (h_i + h_G) c_{i,L}$$

$$1/H_{e,jw}(T) = \ 1/H_{e,jw}(298\ K) * \exp\left(\frac{-d\ \ln k_H}{d(\frac{1}{T})} * \left(\frac{1}{T} - \frac{1}{298} \right) \right)$$

➤ Mass transfer coefficients

Diffusion coefficient

$$D_{iw,L} = \frac{7.4 \times 10^{-8} T(\emptyset\ M_w)^{0.5}}{\mu_L v_i^{0.6}}$$

$$D_{ij,G} = \frac{1 \times 10^{-7} T^{1.75} \left(\frac{1}{M_i} - \frac{1}{M_j} \right)}{p(v_i^{1/3} + v_j^{1/3})^2}$$

Mass transfer coefficient

$$k_G = \frac{A}{RT}\ (R_{eG})^{0.7}\ (S_{cG})^{1/3}\ \left(ad_p \right)^{-2.0} (aD_{kG})$$

$$k_{L,k} = 0.0051\ (R_{eL})^{2/3}(S_{cL})^{-0.5}(a_p d_p)^{0.4}(\frac{\mu_L g}{\rho_L})^{1/3}$$

➤ Numerical solution Equations

$$X_{MDEA,j} = \ X_{MDEA,in} - \frac{v_B Z_T}{H_{T,CO2}} \sum_{i=0}^{NC+1} H_{ji} E_i\ (x_{CO2,i} - x_{CO2,e})$$

$$X_{kj} = \ X_{kin} + \frac{Z_T}{H_{T,k}} \sum_{i=0}^{NC+1} H_{ji}\ (x_{k,i} - x_{k,B})$$

$$T_L = T_{L,out} + \frac{G C_{pG}}{L C_{pL}} \left[(T_G - T_{G,in}) \right] - (-\Delta H_{rx}) \frac{G_{in}}{L C_{pL}} [Y_{CO2,in} - Y_{CO2}]$$

$$T_{G,j} = \ T_{G,out} - N_G \sum_{m=1}^{NC+2} H_{jm}\ (T_{G,m} - T_{L,m})$$

$$H_{T,CO2} = \frac{L_{in}}{A k_{L,CO2} aC}\ , \ \ H_{T,k} = \frac{L_{in}}{A k_{L,k} aC}\ \ , \ \ N_G = \frac{h_G a Z_T}{C_{pG} G}$$

Removal percentage $= 1 - \frac{Y_{CO2,out}}{Y_{CO2,in}}$

APPENDIX C

ABSORPTION SIMULATION FLOW CHART

```
                    ┌──────────────┐
                    │    Start     │
                    └──────────────┘
                           │
                           ▼
              ╱─────────────────────────╲
             ╱  Input data and constant  ╲
             ╲       parameters          ╱
              ╲─────────────────────────╱
                           │
                           ▼
           ┌──────────────────────────────┐
           │  First trial of concentration │
           │  and temperature distribution │
           └──────────────────────────────┘
                           │
                           ▼
           ┌──────────────────────────────┐
           │    Physical and chemical      │
           │        properties             │
           └──────────────────────────────┘
                           │
                           ▼
           ┌──────────────────────────────┐
           │  Solving of material balance  │
           │         equations             │
           └──────────────────────────────┘
                           │
                           ▼
           ┌──────────────────────────────┐
           │  New value of concentration   │
           │  distribution at the column   │
           └──────────────────────────────┘
                           │
                           ▼
           ┌──────────────────────────────┐
           │  New value of concentration   │
           │  distribution at the column   │
           └──────────────────────────────┘
                           │
                           ▼
           ┌──────────────────────────────┐
           │  Deviation= new value – old   │
           │            value              │
           └──────────────────────────────┘
                           │
                           ▼
   No      ╱─────────────────────────╲
 ◄─────────  Deviation < toll
           ╲─────────────────────────╱
                           │
                           ▼
           ┌──────────────────────────────┐
           │   Solving of energy balance   │
           │         equations             │
           └──────────────────────────────┘
                           │
                           ▼
           ┌──────────────────────────────┐
           │  New value of temperature     │
           │  distribution at the column   │
           └──────────────────────────────┘
                           │
                           ▼
           ┌──────────────────────────────┐
           │  Deviation= new value – old   │
           │            value              │
           └──────────────────────────────┘
                           │
                           ▼
           ╱─────────────────────────╲
           ╲  Deviation < toll       ╱
           ╲─────────────────────────╱
                           │
                Yes        ▼
           ┌──────────────────────────────┐
           │    Efficiency estimation      │
           └──────────────────────────────┘
                           │
                           ▼
                    ┌──────────────┐
                    │     End      │
                    └──────────────┘
```

APPENDIX D

LISTING MATLAB PROGRAM

D.1 ABSORPTION PROGRAM

```
clc;
clear;
Z=[0 0.0641299257 0.2041499093 0.395350391 0.604649609
0.7958500907 0.9358700743 1];%column Hieght
H=[0   0.0247375144400  0.013258719820   0.021034356730
0.015779720290   0.019036721340   0.017385669590 0.01785714286
    0   0.0448926626800   0.120649732800   0.096280176310
0.110966975200   0.102247163600   0.106578334600  0.10535211360
    0  -0.0081407677420   0.079997635790   0.189041649800
0.161144336400   0.175394015200   0.168715959500  0.17056134620
    0   0.0042540825490  -0.014480830960   0.101245955600
0.224366717500   0.198597448100   0.208933602400 0.20622939730
    0  -0.0027042050730   0.007631949207  -0.018137320210
0.104983441700   0.220710228300   0.201975314800 0.20622939730
    0   0.0018453866940  -0.004832668923   0.009417009802 -
0.018480303600   0.090563710460   0.178702114000 0.17056134620
    0  -0.0012262209860   0.003104950016  -0.005608861643
0.009071935260  -0.015297619250   0.060459450970 0.10535211260
    0   0.0004714732641  -0.001179578486   0.002077422571 -
0.003177213868   0.004598423035  -0.000880371582 0.01785714286];




TLI= 325; %liquid feed temperature (K)
PT=41.06; %absorber pressure(atm)
TGI=298;%gas feed temperature (K)

%column details
ZT=1410;%hieght of column (cm)
DC=410;%diameter of column (cm)
DP=5;%packing size (cm)
AP=2*4.5;%packing specific area(cm2/cm3)
AC=1/4*3.14*(DC^2);%cross sectional area of tower(cm2)

%Liquid stream
%mass fraction of component in the liquid stream(gr/gr)
WMDIN=0.45;%MDEA
WMHIN=0.00133;%MDEAH+
WKIN=0.05;%glyk
WKOIN=0.0;%glyCOO
WCDIN=8.4947e-007;%CO2
WNIN=0.0;%N2
WMIN=0.0;%CH4
WWIN=1-(WMDIN+WMHIN+WKIN+WCDIN+WNIN+WMIN);
LLAKGA=1016300;%flow rate liquid feed(Kg/hr)
LLAKG=LLAKGA/3.6;%flow rate liquid(g/s)
Water=WWIN*LLAKG/18;
%MOLECULAR WEIGHT
```

```
MWCD=44;%molecular weight CO2(gr/mol)
MWN=28;%molecular weight N2(gr/mol)
MWM=16;%molecular weight CH4(gr/mol)
MWMD=119.16;%molecular weight MDEA(gr/mol)
MWMH=181.176;%molekular weight R-HCO3(gr/mol)
MWK=113.157;%molecular weight glyk(gr/mol)
MWW=18;%solvent molecular weight(gr/mol)
XMDIN=(WMDIN/MWMD)/((WMDIN/MWMD)+(WMHIN/MWMH)+(WKIN/MWK)+(WWIN/MWW
));
XMHIN=(WMHIN/MWMH)/((WMDIN/MWMD)+(WMHIN/MWMH)+(WKIN/MWK)+(WWIN/MWW
));
XKIN=(WKIN/MWK)/((WMDIN/MWMD)+(WMHIN/MWMH)+(WKIN/MWK)+(WWIN/MWW));
XWIN=(WWIN/MWW)/((WMDIN/MWMD)+(WMHIN/MWMH)+(WKIN/MWK)+(WWIN/MWW));
MWL=XMDIN*MWMD+XMHIN*MWMH+XKIN*MWK+XWIN*MWW;
%component densitty
dMDIN=1.038;%density of MDEA (gr/cm3)
dMHIN=1.353;%density of MDEAH+(gr/cm3)
dKIN=1.9594;%density of glyk(gr/cm3)
dCDIN=0.77;%density of CO2(gr/cm3)
dNIN=0.125;%densitay of N2 (gr/cm3)
dMIN=0.655;%density of CH4 (gr/cm3)
dWIN=0.998;%density of water(gr/cm3)


RHOL = 1/(WMDIN/dMDIN+WMHIN/dMHIN+WKIN/dKIN+WWIN/dWIN);
C = RHOL/MWL;
ZT=3*ZT;
%concenteration of component in lean solution feed(mol/cm3)
CMDIN=(WMDIN/MWMD)*RHOL;
CMHIN=(WMHIN/MWMH)*RHOL;
CKIN=(WKIN/MWK)*RHOL;
CCDIN=(WCDIN/MWCD)*RHOL;
CNIN=(WNIN/MWN)*RHOL;
CMIN=(WMIN/MWM)*RHOL;
CWIN=(WWIN/MWL)*RHOL;
LLA=LLAKG/(RHOL);%rate lean solution (cm3/s)
LA=LLAKG/(AC*RHOL);%superficial velocity of liquid in the tower
(cm/s)
LM=LLAKGA/MWL;% molar flow rate of liquid in the tower(Kmol/hr)
LM=LM/3.6;%(mol/s)



%GAS STREAM FEED(mol/mol)
YCDIN=0.1931;
YNIN=0.0133;
YMIN=0.7936;
MWG=YCDIN*MWCD+YNIN*MWN+YMIN*MWM;
GA=336520; %flow rate of gas (kg/hr)
G=GA/3.6;%flow rate of gas (g/s)
GM=GA/MWG;
GM=GM/3.6;%(mol/s)
RM=LM/GM; % liquid ,gas flow rate ratio
NMD=1;
NMH=1;
%thermal properties
CPG=2.22;%gas stream heat capacity(J/g K)
CPL=4.185;%liquid stream heat capacity(J/g K)
KDG=0.0343;%thermal conductivity of gas stream(W/M.K)
```

73

```matlab
HRX=-200;%heat of reaction(j/mol)
R=82.057;%gas constant(cm3.atm/mol.k)


XMDIN=CMDIN/C;
XMHIN=CMHIN/C;
XKIN=CKIN/C;
XCDIN=CCDIN/C;
XNIN=CNIN/C;
XMIN=CMIN/C;
XMD(1)=XMDIN;
XMH(1)=XMHIN;
XCD(1)=XCDIN;
XN(1)=XNIN;
XM(1)=XMIN;
XXMD(1)=XMDIN;
XXMH(1)=XMHIN;
XXCD(1)=XCDIN;
XXN(1)=XNIN;
XXM(1)=XMIN;


TLN(1)=TLI;
TGN(1)=TGI+25;
TGN(8)=TGI;
TLN(8)=TLI+31;



EM=0.01;
ey=0.01;
eym=1;
ir=0;
TRM=10;
TM=1;

for i=2:7
    TLN(i)=TLN(1)+Z(i)*(TLN(8)-TLN(1));
    TGN(i)=TGN(1)+Z(i)*(TGN(8)-TGN(1));
end



while eym > ey
    ir=ir+1;
    YYCD(1)=(0.01+(ir-1)*0.001)*YCDIN;
    XXMD(8)=XXMD(1)-(YCDIN-YYCD(1))*NMD/RM;
    XXCD(8)=0.0001;
    XXN(8)=0.000001;
    XXM(8)=0.00001;
    XXMH(8)=XMHIN+NMH*(XMDIN-XXMD(8))/NMD;

    for i=2:7
        XXMD(i)=XXMD(1)+Z(i)*(XXMD(8)-XXMD(1));
        XXCD(i)=XXCD(1)+Z(i)*(XXCD(8)-XXCD(1));
        XXM(i)=XXM(1)+Z(i)*(XXM(8)-XXM(1));
        XXN(i)=XXN(1)+Z(i)*(XXN(8)-XXN(1));
        XXMH(i)=XMHIN+NMH*(XMDIN-XXMD(i))/NMD;
    end
```

```
        ERM=1;
        Count=0;
         for j=2:8
                SIGMAMD=0;
                SIGMACD=0;
                SIGMAN=0;
                SIGMAM=0;




        while ERM > EM
            Count=Count+1;
            SE=0;
            XXMDI(1)=XXMD(1);
            TLI(1)=TLN(1);
            XXMDI(j)=XXMD(j);

            for i=1:8
                TG=TGN(j-1);
                TL=TLN(j-1);
                TI=(TG+TL)/2;
                TF=(TI+TL)/2;
                [K1,K2,K3,K4,K5,k2,k6]=EQU( TL,TG,CWIN);
                [ DCD,DN,DM,KLCD,KLM,KLN,HTUCD,HTUM,HTUN ] =
KL(TL,TG);
                XXMH(i)=XXMH(1)-NMH*(XXMD(i)-XXMD(1))/NMD;
                LT =Water +
LM*(XXMD(i)+XXMH(i)+XXCD(i)+XXN(i)+XXM(i));
                XMD(i)=LM*XXMD(i)/LT;
                XMH(i)=LM*XXMH(i)/LT;
                XN(i)=LM*XXN(i)/LT;
                XM(i)=LM*XXM(i)/LT;
                CMD0=XMD(i)*C;
                CN0=XN(i)*C;
                CM0=XM(i)*C;
                CMH0=XMH(i)*C;
                CCDE=CMH0^2/(CMD0*K1*CWIN);
                XCDE= CCDE/C;
                XCD(i)=XCDE;
                XXCD(i)=LT*XCD(i)/LM;
                XXCDE(i)= XXCD(i);
                CCD0=XCD(i)*C;

                YYCD(i)=YYCD(1)-RM*(XXMD(i)-XXMD(1))/NMD;
                YYN(i)=YNIN;
                YYM(i)=YMIN;

                kov=(k2*CMD0)+(k6*CKIN);
                Ha=(DCD*kov)/KLCD^2;
                E=(1+Ha)^(1/2);
                [ HCD,HN,HM ]
=HE(TG,TL,CMD0,CMH0,CKIN,CWIN,CCD0,K1,K2,K3,K4,K5 );
                if YYCD(i)<0
                    YYCD(i)=0;
                end
```

```
                        YYCDN=YYCD(i);
                        YYNN=YYN(i);
                        YYMN=YYM(i);
                        GT=GM*(YYCDN+YYNN+YYMN);
                        if YYCD(i)==0
                            CCDS=0;
                            XCDS=0;
                            YCD(i)=0;

                        else
                            YCD(i)=GM*YYCD(i)/GT;
                            CCDS=YCD(i)*PT/HCD;
                            XCDS=CCDS/C;
                            CDS=CCDE/CCDS;
                            XCDE=CCDE/C;
                            XCD(i)=XCDE;
                            RB=(1-XCDE/XCDS)*E;
                            SIGMAMD=SIGMAMD+H(i,j)*RB*CCDS;
                        end

                            YN(i)=GM*YYN(i)/GT;
                            YM(i)=GM*YYM(i)/GT;
                            YCDN=YCD(i);
                            YNN=YN(i);
                            YMN=YM(i);
                            [ KGCD,KGM,KGN ,MUG] = KG( G,YCDN,YNN,YMN,TG );
                            XNS=((KGN*YN(i)*PT+KLN*CN0)/(KLN+KGN*HN))/C;
                            XNN=XN(i);
                            XMS =((KGM*YM(i)*PT+KLM*CM0)/(KLM+KGM*HM))/C;
                            XMM=XM(i);

                                if XN(i)>XNS
                                    XN(i)=XNS;
                                else
                                    SIGMAN=SIGMAN+H(i,j)*(XNS-XN(i));
                                end

                                if XM(i)>XMS
                                    XM(i)=XMS;
                                else
                                    SIGMAM=SIGMAM+H(i,j)*(XMS-XM(i));
                                end
                end

                        XXMD(j)=XXMD(1)-NMD*ZT*SIGMAMD/HTUCD;
                        XXMH(j)=XXMH(1)-NMH*(XXMD(j)-XXMD(1))/NMD;
                        XXCD(j)=XXCDE(j);
                        XXN(j)=XN(1)+NMD*ZT*SIGMAN/HTUN;
                        XXM(j)=XM(1)+NMD*ZT*SIGMAM/HTUM;
                        LT =Water +
LM*(XXMD(j)+XXMH(j)+XXCD(j)+XXN(j)+XXM(j));
                        XMD(j)=LM*XXMD(j)/LT;
                        XMH(j)=LM*XXMH(j)/LT;
                        XN(j)=LM*XXN(j)/LT;
                        XM(j)=LM*XXM(j)/LT;
                        YYCD(j)=YYCD(1)-RM*(XXMD(j)-XXMD(1))/NMD;
                        YYN(j)=YNIN;
```

```matlab
                        YYM(j)=YMIN;
                        GT=GM*(YYCD(j)+YYN(j)+YYM(j));
                        YCD(j)=YYCD(j)*GM/GT;
                        YN(j)=YYN(j)*GM/GT;
                        YM(j)=YYM(j)*GM/GT;
                        GTW=GT*(YCD(j)*MWCD+YN(j)*MWN+YM(j)*MWM);
                        ERM=SE;

        end
        ERM=1;
                while TRM > TM
                  SIGMAT=0;
                  TGI(j)=TGN(j);
                  TE=0;
                  for i=1:8
                        TG=TGN(i);
                        TL=TLN(i);
                        TI=(TG+TL)/2;
                        TF=(TI+TL)/2;
                        YCDN=YCD(j);
                        YNN=YN(j);
                        YMN=YM(j);
                        [ KGCD,KGM,KGN ,MUG] = KG( G,YCDN,YNN,YMN,TG
);
                        [ DCD,DN,DM,KLCD,KLM,KLN,HTUCD,HTUM,HTUN ] =
KL(TL,TG);
                        GTW=GT*(YCD(j)*MWCD+YN(j)*MWN+YM(j)*MWM);
                        PR=CPG*MUG/KDG;
                        RHOG=MWG*PT/(R*TG);
                        SC=MUG/(RHOG*DM);
                        HG=KLM*SC^(2/3)*RHOG*CPG/PR^(2/3);
                        NG=HG*AP*ZT/(CPG*GTW);
                        SIGMAT=SIGMAT+H(i,j)*(TGN(i)-TLN(i));
                        L=G+LLAKG-GTW;
                    end
                TGN(j)=TGN(1)+NG*SIGMAT;
                TLN(j)=TLN(8)+(GTW*CPG/(L*CPL))*((TGN(j)-TGN(8)))-
((-HRX)*GM/(L*CPL))*(YCDIN-YCD(j));
                TE=TE+abs((TGN(j)-TGI(j))/TGN(j));
                TRM=TE;

         end

        TRM=10;

         if Count == 1000
            disp(['Error=',num2str(ERM)]);
            ERM=0.5*EM;
            disp('can not be solved');

         end

    end
    eym=abs((YYCD(8)-YCDIN)/YCDIN);

end
```

```matlab
  for j=1:8
      CMD(j)=XMD(j)*C;
      CMH(j)=XMH(j)*C;


  end

RR = LM*(XXMD(1)-XXMD(8));
REC=RR/(GM*YCDIN);
YYCD1=YYCD(1);
TOT=YCD(1)+YN(1)+YM(1);
YCDOUT=YCD(1)/TOT;
YNOUT=YN(1)/TOT;
YMOUT=YM(1)/TOT;
MWGOUT=YCDOUT*MWCD+YNOUT*MWN+YMOUT*MWM;
WGCDOUT=YCDOUT*MWCD/MWGOUT;
WGNOUT=YNOUT*MWN/MWGOUT;
WGMOUT=YMOUT*MWM/MWGOUT;
ZT=ZT/3;

disp('   ');
disp('   ');
disp('                                          DATA CO2 ABSORBER
');
disp('   ');
disp(['        inlet gas stream flow rate (kg/jam)
:',num2str(real(G))]);

disp('   ');
disp('
_____
_____   ');
disp('   ');
disp('          1. mole fraction of outlet gas stream');
disp('
_____');
disp(['          CO2:',num2str(YCDOUT)]);
disp(['          N2 :',num2str(YNOUT)]);
disp(['          CH4:',num2str(YMOUT)]);


GTM=GM*(YCDOUT*MWCD+YNOUT*MWN+YMOUT*MWM);%flow rate of exit gas
(gr/s)
disp(['        outlet gas stream flow rate(kg/jam)
:',num2str(real(GTM))]);
MWW=18;
MDML=XMD(8)*MWMD+XMH(8)*MWMH+XKIN*MWK+((1-XMD(8)-XMH(8)-
XKIN)*MWW);
XMDOUT=XMD(8);
XMHOUT=XMH(8);
XKOUT=XKIN;
XCDOUT=XCD(8);
XNOUT=XN(8);
XMOUT=XM(8);
WMDOUT=XMD(8)*MWMD/MDML
WMHOUT=XMH(8)*MWMH/MDML;
```

```matlab
WKOUT=XKIN*MWK/MDML;
WCDOUT=XCD(8)*44/MDML;
WNOUT=XN(8)*28/MDML;
WMOUT=XM(8)*16/MDML;
WWOUT=(1-(WMDOUT+WMHOUT+WKOUT));
WWOUT=WWIN*LLAKGA;
LLKG=G+LLAKGA-GTM;

disp([' BMLB =',num2str(MDML)]);
disp('  ');
disp('              2. Mass fraction of out put liquid flow ');
disp('
_____');
disp(['              MDEA:',num2str(WMDOUT)]);
disp(['              R-HCO3:',num2str(WMHOUT)]);
disp(['              GLYK :',num2str(WKOUT)]);
disp(['              CO2  :',num2str(WCDOUT)]);
disp(['              N2   :',num2str(WNOUT)]);
disp(['              CH4  :',num2str(WMOUT)]);
disp('  ');
disp(['         Solution mass flow rate:',num2str(LLKG)]);
disp('  ');


MMHOUT=WMHOUT*LLKG;
NMHOUT=MMHOUT/MWMH;
NCO2OUT=NMHOUT;
MCO2OUT=NCO2OUT*MWCD;
MCO2IN=WCDIN*LLAKGA;
MCDOUT=WCDOUT*G;
MCDIN=WCDIN*G;
EF2=(MCDOUT-MCDIN)/MCDIN*100;
EF=(MCO2OUT-MCO2IN)/MCO2IN*100;
YYCD8=YYCD(8)
YYCD1=YYCD(1)
Rec = 100*(YYCD(8)-YYCD(1))/YYCD(8);
disp('  ');
disp('  ');
disp([' Persen Recovery:  ',num2str(Rec),' %']);
disp('  ');
disp('  ');
disp('                              4. liquid concentration
distribution');
disp('_____');
disp(['  zz  ' , '      MDEA  ' , ',      R-HCO3  ',]);
disp('_____');

for i=1:8
    ZZB(i)=Z(i)*ZT;%column hieght (m)
end
disp([num2str(real(ZZB(1))),'            ',num2str(real(XMD(1))),'
',num2str(real(XMH(1))),'     ',num2str(real(XCD(1))),'     ']);
disp([num2str(real(ZZB(2))),'    ',num2str(real(XMD(2))),'  ,'
',num2str(real(XMH(2))),'     ',num2str(real(XCD(2))),'     ']);
disp([num2str(real(ZZB(3))),'   ',num2str(real(XMD(3))),'  ,'
',num2str(real(XMH(3))),'     ',num2str(real(XCD(3))),'      ']);
disp([num2str(real(ZZB(4))),'    ',num2str(real(XMD(4))),'  ,'
',num2str(real(XMH(4))),'      ',num2str(real(XCD(4))),'      ']);
```

```
disp([num2str(real(ZZB(5))),'    ',num2str(real(XMD(5))),'  ',' 
',num2str(real(XMH(5))),'        ',num2str(real(XCD(5))),'      ']);
disp([num2str(real(ZZB(6))),'  ',num2str(real(XMD(6))),'  ',' 
',num2str(real(XMH(6))),'        ',num2str(real(XCD(6))),'      ']);
disp([num2str(real(ZZB(7))),'  ',num2str(real(XMD(7))),'  ',' 
',num2str(real(XMH(7))),'        ',num2str(real(XCD(7))),'      ']);
disp([num2str(real(ZZB(8))),'        ',num2str(real(XMD(8))),' 
',num2str(real(XMH(8))),'        ',num2str(real(XCD(8))),'      ']);




 subplot(1,2,1)
 plot(ZZB,XMD,'-.k',ZZB,XMH,':k')
 title ('mole fraction profile vs column hieght (liquid)')
 xlabel('column hieght(m)')
 ylabel('mole fraction')
 legend('MDEA','R-HCO3',1)

subplot(1,2,2)
plot((Z),YCD,'-.k')

xlabel('Axial position')
ylabel('mole fraction')
legend('CO2',1)
```

D.2 Functions program Listing
- Equilibrium constants and reaction kinetics constant (EQU)

```
function [K1,K2,K3,K4,K5,k2,k6]=EQU( TL,TG,CWIN)
TI=(TG+TL)/2;% interface temperature in tower(K)
TF=(TI+TL)/2;%film temperture(K)
K2=((exp((-12091.1/TF)-
(36.7816*log(TF))+235.482)))*CWIN;%equilibrium constant for
rection (2.57)(-)
K3=((exp((-12431.7/TF)-
(35.4819*log(TF))+220.067))/1000)*CWIN;%equilibrium constant for
rection (mole/cm3)(2.58)
K4=((exp((-423.98/TF)-9.4165))/1000)*CWIN;%equilibrium constant
for rection (mole/cm3)(2.59)
K5=((exp((-13445.9/TF)-
(22.4773*log(TF))+140.932))/1000)*CWIN;%equilibrium constant for
rection (2.60)(mole/cm3)
K1=1000*K2/K4;%equilibrium constant for rection (cm3/mole)(2.56)
k2=(1.78*10^10*exp(-6441.9/TF))*1000;%reaction rate constant
(cm3/mole.s)
k6=(2.81*10^10*exp(-5800/TF))*1000;%reaction rate constant
(cm3/mole.s)

end
```
- Liquid mass transfer coefficient

```
function [ DCD,DN,DM,KLCD,KLM,KLN,HTUCD,HTUM,HTUN ] = KL(TL,TG)
TI=(TG+TL)/2;%interface temperature in the tower(K)
```

```matlab
TF=(TI+TL)/2;%film temperature in the tower(K)
RHOL=1.042; %densitas liquid (g/cm3)
C=0.0333;%molar density of solution (mol/cm3)


%column details
ZT=1410;%hieght of column (cm)
DC=410;%diameter of column (cm)
DP=5;%packing size (cm)
AP=4.5;%packing specific area(cm2/cm3)
AC=1/4*3.14*(DC^2);%cross sectional area of tower(cm2)


%liquid stream
LLAKGA=1016300;%flow rate liquid feed(Kg/hr)
LLAKG=LLAKGA/3.6;%flow rate liquid(g/s)
LLA=LLAKG/(RHOL);%rate lean solution (cm3/s)
LA=LLAKG/(AC*RHOL);%superficial velocity of liquid in the tower
(cm/s)


%molecular volume (cm3/gmol)
VCD=34;
VN=31.2;
VM=24;
PHI=2.6; %assosiation factor
MWL=18; %molecular weight (gr/gmol)
MUA=0.003393*exp(1693.86/TF); %viscosity (gr/m.s)
%Diffusivity (cm2/s)
DCD=0.000000074*TF*(PHI*MWL)^0.5/(MUA*VCD^0.6);
DN=0.000000074*TF*(PHI*MWL)^0.5/(MUA*VN^0.6);
DM=0.000000074*TF*(PHI*MWL)^0.5/(MUA*VM^0.6);


SIGMAL=20; %surface tension of the liquid phase(dyne/cm,gr/s2)
SIGMAR=0.85; %reduced surface tension(dyne/cm,gr/s2)
%scmidth number
NSCCD=MUA*0.01/(RHOL*DCD);
NSCN=MUA*0.01/(RHOL*DN);
NSCM=MUA*0.01/(RHOL*DM);
GG=980; %acceleration of gravity (cm/s2)
NLAT=RHOL*LA/(0.01*AP*MUA); %
NLRG=AP*LA^2/(GG); % Froude number
NLSG=RHOL*LA^2/(SIGMAL*AP); %Weber number
FCT=-1.45*SIGMAR^0.75*NLAT^0.1*NLRG^-0.05*NLSG^0.2;
AAA=AP*(1-exp(FCT));%a'
AA=AAA*100;
NLAA=NLAT*AP/AAA; %ReL'
NRMUA=RHOL/(0.01*MUA*GG); %
ATD=AP*DP; %ap*dp
%mass transfer coeff  (cm/sec)
KLCD=0.0051*NLAA^(2/3)*NSCCD^(-0.5)*ATD^0.4*NRMUA^(-1/3);
KLN=0.0051*NLAA^(2/3)*NSCN^(-0.5)*ATD^0.4*NRMUA^(-1/3);
KLM=0.0051*NLAA^(2/3)*NSCM^(-0.5)*ATD^0.4*NRMUA^(-1/3);


%Height of a transfer unit  (cm)
HTUCD=LA/(KLCD*AAA);
HTUN=LA/(KLN*AAA);
HTUM=LA/(KLM*AAA);
```

```matlab
end
```

- Gas mass transfer coefficient

```matlab
function [ KGCD,KGM,KGN ,MUG] = KG( G,YCDN,YNN,YMN,TG )
ZT=1410;%hieght of column (cm)
DC=410;%diameter of column (cm)
DP=5;%packing size (cm)
AP=4.5;%packing specific area(cm2/cm3)
AC=1/4*3.14*(DC^2);%cross sectional area of tower(cm2)
PT=41.65;%Column pressure
R=82.057;%gas constant(cm3.atm/mol.k)
%Gas stream
%MOLECULAR WEIGHT
MWCD=44;%molecular weight CO2(gr/mol)
MWN=28;%molecular weight N2(gr/mol)
MWM=16;%molecular weight CH4(gr/mol)
MWG=YCDN*MWCD+YNN*MWN+YMN*MWM;
%molecular volume(cm3/mol)
VCDG=26.9;
VNG=17.9;
VMG=24.42;
%viscosity ( gr/cm.s)
MUCD=(10^(578.08*(1/TG-1/185.24)))/100;
MUN=(10^(90.30*(1/TG-1/46.14)))/100;
MUM=(10^(114.14*(1/TG-1/57.60)))/100;

YMCD=YCDN*MWCD/MWG;
YMN=YNN*MWN/MWG;
YMM=YMN*MWM/MWG;

MUG=MUCD*YMCD+MUN*YMN+MUM*YMM;%gas viscosity (cps , gr/cm.s)

% diffusivity of CO2
DG1=10^-
3*TG^1.75*(1/MWCD+1/MWN)^0.5/(PT*((VCDG^(1/3))+VNG^(1/3))^2);%diff
usivity of CO2 against N2(cm2/s)
DG2=10^-
3*TG^1.75*(1/MWCD+1/MWM)^0.5/(PT*((VCDG^(1/3))+VMG^(1/3))^2);%diff
usivity of CO2 against CH4(cm2/s)
DM=(1-YCDN)/(YNN/DG1+YMN/DG2);%diffusivity of CO2 against gas
mixer  (cm2/s)
RHOG=MWG*PT/(R*TG);%density of gas at the column
NREG=G/(AC*MUG*AP);% reynold nymber for gas phase
NSCG=MUG/(RHOG*DM);% schmidt number
KGCD=(5.23/(R*TG))*NREG^0.7*NSCG^(1/3)*(AP*DP)^-2*(AP*DM);%mass
transfer coeff (mol/cm2.s.atm)


% diffusivity of N2
```

```matlab
DG1=10^-
3*TG^1.75*(1/MWN+1/MWCD)^0.5/(PT*((VNG^(1/3))+VCDG^(1/3))^2);%diff
usivity of N2 against CO2(cm2/s)
DG2=10^-
3*TG^1.75*(1/MWN+1/MWM)^0.5/(PT*((VNG^(1/3))+VMG^(1/3))^2);%diffus
ivity of N2 against CH4(cm2/s)
DM=(1-YNN)/(YCDN/DG1+YMN/DG2);%diffusivity of N2 against gas mixer
(cm2/s)
RHOG=MWG*PT/(R*TG);%density of gas at the column
NREG=G/(AC*MUG*AP);% reynold nymber for gas phase
NSCG=MUG/(RHOG*DM);% schmidt number
KGN=(5.23/(R*TG))*NREG^0.7*NSCG^(1/3)*(AP*DP)^-2*(AP*DM);%mass
transfer coeff (mol/cm2.s.atm)


% diffusivity of CH4
DG1=10^-
3*TG^1.75*(1/MWM+1/MWN)^0.5/(PT*((VMG^(1/3))+VNG^(1/3))^2);%diffus
ivity of CH4 against N2(cm2/s)
DG2=10^-
3*TG^1.75*(1/MWM+1/MWCD)^0.5/(PT*((VMG^(1/3))+VCDG^(1/3))^2);%diff
usivity of CH4 against CO2(cm2/s)
DM=(1-YMN)/(YNN/DG1+YCDN/DG2);%diffusivity of CH4 against gas
mixer  (cm2/s)
RHOG=MWG*PT/(R*TG);%density of gas at the column
NREG=G/(AC*MUG*AP);% reynold nymber for gas phase
NSCG=MUG/(RHOG*DM);% schmidt number
KGM=(5.23/(R*TG))*NREG^0.7*NSCG^(1/3)*(AP*DP)^-2*(AP*DM);%mass
transfer coeff (mol/cm2.s.atm)




end
```

- Henry constant

```matlab
function [ HCD,HN,HM ]
=HE(TG,TL,CMD0,CMH0,CKIN,CWIN,CCD0,K1,K2,K3,K4,K5)
TI=(TG+TL)/2;%interface temperature in the tower(K)
TF=(TI+TL)/2;%film temperature in the tower(K)
CMD=CMD0*1000;%MDEA concentration in liquid feed stream (kmol/m3)
CMH=CMH0*1000;%R-MDEA concenteration in liquid feed stream
(kmol/m3)
CW=CWIN*1000;%water concenteration in liquid feed stream (kmol/m3)
CK=CKIN*1000;%k concenteration in liquid feed stream (kmol/m3)
CCO2=CCD0*1000;%CO2 concenteration in liquid feed stream (kmol/m3)
CHCO3=CMH0;%HCO3 concenteration in liquid feed stream (kmol/m3)
CH=(K2*CCO2*CWIN)/(CHCO3);%H concenteration in liquid feed stream
(kmol/m3)
CCO3=K3*CHCO3*1000/(CH);%CO3 concenteration in liquid feed stream
(kmol/m3)
```

```
COH=K5*CWIN*1000/CH;%OH concenteration in liquid feed stream
(kmol/m3)
CGLY=CK;%GLY concenteration in liquid feed stream (kmol/m3)
%henry inverse constant pure water at 298(kmole/m3.atm))
KHOCD=3.6*10^-2;
KHON=6.1*10^-4;
KHOM=140*10^-4;


%enthalby part constant(k)
dCD=2200;
dN=1300;
dM=1600;


%henry inverse constant pure water at temperature
(T)(kmole/m3.atm)
KHCD=KHOCD*exp(dCD*((1/TF)-(1/298)));
KHN=KHON*exp(dN*((1/TF)-(1/298)));
KHM=KHOM*exp(dM*((1/TF)-(1/298)));


%henry constant pure water at temperature (T)(m3.pa/kmole)
HWCD=101325/KHCD;
HWN=101325/KHN;
HWM=101325/KHM;


%hG at T=298 K(m3/kmole)
HGOCD=-1.72*10^-5;
HGON=-1*10^-6;
HGOM=2.2*10^-6;


%parameter hT of gas (m3/kmole.K)
HTCD=-3.38*10^-7;
HTN=-6.05*10^-7;
HTM=-5.24*10^-7;


%hG,o of gas at temperture T(m3/kmole)
HGCD=HGOCD+HTCD*(TF-298.15);
HGN=HGON+HTN*(TF-298.15);
HGM=HGOM+HTM*(TF-298.15);
HMHPLUS=0.041;% ion plus concenteration, MDEAH+ (m3/kmol)
HKPLUS=0.092;
HCO3MIN=0.1423;%ion plus concenteration, CO3- (m3/kmol)
HHCO3MIN=0.0967;%ion plus concenteration, HCO3- (m3/kmol)
HOHMIN=0.061;
HGLYMIN=0.0413;
%hI constant in MDEA(m3/kmol)
SUMCD=(HMHPLUS+HGCD)*CMH+(HKPLUS+HGCD)*CK+(HCO3MIN+HGCD)*CCO3+(HOH
MIN+HGCD)*COH+(HHCO3MIN+HGCD)*CHCO3+(HGLYMIN+HGCD)*CGLY;
SUMN=(HMHPLUS+HGN)*CMH+(HKPLUS+HGN)*CK+(HCO3MIN+HGN)*CCO3+(HHCO3MI
N+HGN)*CHCO3+(HOHMIN+HGN)*COH+(HGLYMIN+HGN)*CGLY;
SUMM=(HMHPLUS+HGM)*CMH+(HKPLUS+HGM)*CK+(HCO3MIN+HGM)*CCO3+(HHCO3MI
N+HGM)*CHCO3+(HOHMIN+HGM)*COH+(HGLYMIN+HGM)*CGLY;


%henry constant (pa.m3/kmol)
HCDA=HWCD/10^(SUMCD);
HNA=HWN/10^(SUMN) ;
HMA=HWM/10^(SUMM);
```

```
%henry constant (atm.cm3/mol)
HCD=HCDA*(10^6/(101325*10^3));
HN=HNA*(10^6/(101325*10^3));
HM=HMA*(10^6/(101325*10^3));




end
```

CHAPTER 5
CONCLUSION

Based on a simulation model the following points is obtained:

1. In this research a mathematical model of reactive absorption of CO_2 into promoted MDEA with piperazine at packed column has been created. Data for thermodynamic properties and chemical reactions used in the simulation were obtained from previous experimental studies on the MDEA-PZ-CO_2 system.

2. Validation of the mathematical model for the process of absorption of CO_2 by promoted MDEA solution in a packed column has been done on actual data of absorber in an existing natural gas sweetening process in Thailand called Acid Gas Removal Unit (AGRU).which is also using a solvent MDEA and piperazine as a promoter. and obtained the error of 3.723% .

3. A simulation model has been developed with an amino acid promoter, potassium glycinate, instead of piperazine in the same gas feed condition and column configurations and the influence of various operating variables on the performance of the column have been examined theoretically,The following results is conclude:

   - Increase of absorbent flow rate will increase % CO_2 removal. The increase of absorbent flow rate from 914,670 to 1,341,516 kg/hr shift % CO_2 removal from 87.79% to 99.008%

   - It is beneficial for a reactive absorption, to increase feed temperature of gas and liquid stream to some extent for higher CO_2 removal efficiency. The highest CO_2 removal efficiency is 98.89% at lean solution temperature of 365 K compare to 91.6654% CO_2 recovery efficiency when the lean solution feed temperature is 325 K

   - CO_2 removal efficiency increases with increasing of operation pressure of the absorption column. As at pressure of 25 atm the CO_2 removal efficiency for promoter PZ and potassium glycinate are 79.2981%; 71.9556%, respectively.

Meanwhile, at pressure of 45 atm the CO_2 removal efficiency are 97.8957%; 94.276%, respectively.

- Every 1 wt% increasing the Potassium glycinate concentration will enhance the recovery rate by about 4 %. The result also confirmed that the MDEA solvent alone without any activator is not effective in capturing CO_2 since it will leave a large amount of CO_2 in the vented gas.

Suggestions:

- The developed program should be validated against data from other factories to improve the accuracy of the mathematical model.
- Simulation absorber unit is combined with the stripper unit to evaluate the performance of a CO2 removal unit as a whole.

References

Ahmady A, Mohd. Ali Hashim, Mohamed Kheireddine Aroua (2011). "Absorption Of Carbon Dioxide In The Aqueous Mixtures Of Methyldiethanolamine With Three Types Of Imidazolium-Based Ionic Liquids." Fluid Phase Equilibria 309, 76– 82,.

Aliabad Z, H., And Mirzaei, S. (2009)"Removal Of CO2 And H2S Using Aqueous Alkanolamine Solusions." World Academy Of Science, Engineering And Technology Vol:3.

Altway A , S. Susianto, S. Suprapto, Siti Nurkhamidah, Nur Ihda Farihatin Nisa, Firsta Hardiyanto, Hendi Riesta Mulya, Saidah Altway (2015). "Modeling And Simulation Of CO2 Absorption Into Promoted Aqueous Potassium Carbonate Solution In Industrial Scale Packed Column." Bulletin Of Chemical Reaction Engineering & Catalysis: 10 (2),111-124.

Astarita G., Savage D., Bisio A.(1983). "Gas Treating With Chemical Solvents. " Wiley, New York.

Astarita, G. (1961). "Carbon Dioxide Absorption In Aqueous Monoethanolamine Solutions." Chem. Engr. Sci. 16: 202–207.

Austgen, D. M.; Rochelle, G. T.; Chen, C. C. (1989) "A Model Of Vapor-Liquid Equilibria For Aqueous Acid Gas-Alkanolamine Systems Using The Electrolyte-NRTL Equation ". Ind. Eng. Chem. Res., 28 (7), 1060

Bandyopadhyay, Arunkumar Samanta And S. S(2010). "Absorption Of Carbon Dioxide Into Piperazine Activated Aqueous N-Methyldiethanolamine.".

Bishoni, Sanjay (2000). "Carbon Dioxide Absorption And Solution Equilibrium In Piperazine Activated Methyldiethanolamine." ,Dissertation ,The University Of Texas At Austin.

Blauwhoff, P.M.M., Versteeg, G.F., (1984). "A Study On The Reaction Between CO2 And Alkanolamines In Aqueous-Solutions ". Chemical Engineering Science 39 (2), 207–225

Bolhàr-Nordenkampf M, Anton Friedl , Ulrich Koss , Thomas Tork(2004). "Modelling Selective H2S Absorption And Desorption In An Aqueous MDEA-Solution." Chemical Engineering And Processing 43 , 701–715.

Boot-Handford, M. E., Abanades, J. C., Anthony, E. J., Blunt, M. J., Brandani, S., Mac Dowell,N., Fennell, P. S. (2014). "Carbon Capture And Storage Update. Energy And Environmental Science" The Royal Society Of Chemistry.

Brouwer .J.P, P.H.M. Feron, N.A.M. Ten Asbroek. "Amino-Acid Salts For CO2 Capture From Flue Gases." TNO Science & Industry,Department Of Separation Technology,The Netherlands.

BULLIN J .A, JOHN C. POLASEK,STEPHEN T. DONNELLY,(2006). "The Use Of MDEA And Mixtures Of Amines For Bulk CO2 Removal ." Bryan Research And Engineering, Inc,.

Caplow,M,(1968). "Kinetics Of Carbonate Formation And Breakdown, "J.Am.Chem.Soc., 90,6795.

Chacuk, Hanna Kierzkowska-Pawlak And Andrzej (2010). "Kinetics Of Carbon Dioxide Absorption Into Aqueous Mdea Solutions ." Ecological Chemistry And Engineering S: Vol. 17, No. 4,463-475.

Chakravati S, Gupta A, Hunek B. (2001) ." Advanced Technology For The Capture Of Carbon Dioxide From Flue Gases ". 1st National Conference On Carbon Sequestration,Washington DC

Crooks,J.E.,Donellan,J.P (1989)., "Kinetics And Mechanism Of The Reaction Between Carbon Dioxide And Amines In Aqueous Solutions."J,Chem..Soc.Perkin.Trans.II.331.

Danckwerts A.W., (1951). "Significance of Liquid Film Coefficient In Gas Absorption". Ind. Eng. Chem. 43, 1460-1467.

Danckwerts,P.V.(1970) "Gas Liquid Reactions ".Mcgraw Hill,NY

Danckwerts,P.V.(1979) "The Reaction Of CO2 With Ethanolamines,"Chem.Eng.Sci.,34,443.

Daubert, T.E., Danner, R.P. (1985). " Data Com-Pilation Tables Of Properties Of Pure Com-Pounds, Design Institute For Physical Property Data ",AICHE, New York.

Derks, P.W.J., Kleingeld, T.,.(2006). "Kinetics Of Absorption Of Carbon Dioxide In Aqueous Piperazine Solutions." Chemical Engineering Science. , 61 (20), 6837–6854

Devries, Nicholas P (2014). "Co2 Absorption Into Concentrated Carbonate Solutions With Promoters At Elevated Temperatures ." , Dissertation.University Of Illinois At Urbana-Champaign.

Donaldson, T. L. And Y. N. Nguyen (1980). "Carbon Dioxide Reaction Kinetics And Transport In Aqueous Amine Membranes." Ind. Eng. Chem. Fundam. 19: 260–266.

Dubois L. (2013). "Etude De La Capture Du CO2 En Postcombustion Par Absorption Dans Des Solvants Aminés : Application Aux Fumées Issues De Cimenteries ". , Dissertation ,University Of Mons, Belgium.

Dugas, Ross Edward(2009). "Carbon Dioxide Absorption, Desorption, And Diffusion In Aqueous Piperazine And Monoethanolamine." , Dissertation.The University Of Texas At Austin,.

Faramarzi L, Kontogeorgis G., Michelsen M., Thosen K., Stenby E. (2010). "Absorber Model For CO2 Capture By Monoethanolamine. " Ind. Eng. Chem. Res. 49, 3751–3759.

Glasscock,D.A. (1990). "Modelling And Experimental Study Of Carbon Dioxide Absorption Into Aqueous Alkanolamines ".Dissertation, The University Of Texas At Austin.

Glasscock D.A. and Rochelle G.T (1989) " Numerical simulation of theories for gas absorption with chemical reaction". AIChE J., 35(8), 1271-1281.

Haimour N., Bidarian A., Sandall O.C., (1987). " Kinetics Of The Reaction Between Carbon Dioxide And Methyldiethanolamine ". Chem. Eng. Sci., 42, 1393-1398.

Huang , Allan N. Soriano , Alvin R. Caparanga, Meng-Hui Li .(2011) "Kinetics Of Absorption Of Carbon Dioxide In 2-Amino-2-Methyl-L-Propanol +N-Methyldiethanolamine + Water." Journal Of The Taiwan Institute Of Chemical Engineers 42 , 76–85.

Idem R., Wilson M., Tontiwachwuthikul P., Chakma A., Veawab A., Aroonwilas A., Gelowitz D., (2006)." Pilot Plant Studies Of The CO2 Capture Performance Of Aqueous MEA And Mixed MEA/MDEA Solvents At The University Of Regina CO2 Capture Technology Development Plant And The Boundary Dam CO2 Capture Demonstration Plant". Ind. Eng. Chem. Res. 45, 2414-2420.

IEA (2007), World Energy Outlook 2007 - China and India Insights: Executive Summary. Paris, France: OECD/IEA;.

IEA (2004), "Prospects For CO2 Capture And Storage ". Paris, France: OECD/IEA.

IEA GHG (2010), Project Details: CASTOR, "CO2 from Capture To Storage". Www.Co2captureandstorage.Info/Project_Specific.Php?Project_Id=124

IPCC (2005), "Intergovernmental Panel On Climate Change (IPCC) Special Report On Carbon Dioxide Capture And Storage," Cambridge University Press, Cambridge, UK.

IEA GHG (1993), "The Capture of Carbon Dioxide from Fossil Fuel Fired Power Stations. Cheltenham, " UK: IEA GHG; IEA GHG/SR2

Jamal A., Meisen A., Jim Lim C., (2006). "Kinetics Of Carbon Dioxide Absorption And Desorption In Aqueous Alkanolamine Solutions Using A Novel Hemispherical Contactor – I. Experimental Apparatus And Mathematical Modeling ". Chem. Eng. Sci., 61, 6571-6589.

Jensen,A.,Jorgensen,E.,Faurholt,C.,(1954) "Reactions Between Carbon Dioxide And Amine Alcohols. I.Monoethanolamine And Diethanolamine". Act a Chemica Scandinavice,8,1137-1140

Kenarsari, S. D., Yang, D., Jiang, G., Zhang, S., Wang, J., Russell, A. G., Fan, M. (2013)."Review of Recent Advances In Carbon Dioxide Separation And Capture ". RSC Advances: Theroyal Society Of Chemistry.

Kierzkowska-Pawlak H., Chacuk A., (2010). "Kinetics Of Carbon Dioxide Absorption Into Aqueous MDEA Solutions ". Ecol. Chem. Eng. S, 17, 463-475.

Kierzkowska-Pawlak H, Marta Siemieniec, Andrzej Chacuk (2011). "Reaction Kinetics Of Co2 In Aqueous Methyldiethanolamine Solutions Using The Stopped-Flow Technique ." Chemical And Process Engineering: 33 (1), 7-18

King,C.J.,(1966)., "Turbulent Liquid Phase Mass Transfer At A Free Gas-Liquid Interface, ",Ind.Eng.Chem.Fund.,5,1,1-8

Ko J.-J., Li M.-H., (2000). "Kinetics Of Absorption Of Carbon Dioxide Into Solutions Of N-Methyldiethanolamine + Water. "Chem. Eng. Sci., 55, 4139-4147.

Kucka L., Richter J., Kenig E., Gorak A.,(2003). "Determination Of Gas-Liquid Reaction Kinetics With A Stirred Cell Reactor ". Sep. Purif.Technol. 31, 163–175

Kumar, P., Hogendoorn, J., Et Al., (2003a). " Equilibrium Solubility Of CO2 In Aqueous Potassium Taurate Solutions: Part 1. Crystallization In Carbon Dioxide Loaded Aqueous Salt Solutions Of Amino Acids ". Industrial & Engineering Chemistry Research 42 (12), 2832–2840.

Kumar, S., Cho, J. H., & Moon, I. (2014). "Ionic Liquid-Amine Blends And CO2BOLs: Prospective Solvents For Natural Gas Sweetening And CO2 Capture Technology-A Review". International Journal Of Greenhouse Gas Control, 20, 87-116.

L.Mccabe W, Julian C.Smith,Peter Harriot. "Unit Operation Of Chemical Engineering". Mcgraw-Hill Chemical Engineering Series, Fifth Edition .

Grégoire L (2013). "Optimal Design Of A CO2 Capture Unit With Assessment Of Solvent Degradation.", Dissertation. Unversite De Liege,Dissertation

Li L , Gary T. Rochelle(2011). "Amino Acid Solvents For CO2 Absorption." Energy Procedia.In Process.

Little R.J, G. F. Versteeg And W_ P. M. Van Swaaij(1991). "Kinetics Of Co2 With Primary And Secondary Amines In Aqueous Solutions-I. Zwitterion Deprotonation Kinetics For Dea And Dipa Inaqueous Blends Of Alkanolamines." Chemkd Era&Ebng Science, Vol. 47. No. 8, Pp. 2027-2035,.

Little.R.J, G. F. Versteeg And W. P. M. Van Swaaij(1992). "Kinetics Of Co2 With Primary And Secondary Amines In Aqueous Solutions-Ii. Influence Oftemperature On Zwitterion Formation Anddeprotonation Rates." Chemical Engine&Ng Science, Vol. 47, No. 8, Pp. 2037-2943.

Littel R.J., Versteeg G.F., Van Swaaij W.P.M., (1991). "Kinetics Of Carbon Dioxide With Tertiary Amines In Aqueous Solution ". Aiche J., 36, 1633-1640

Mandala.B.P, M. Guhab, A. K. Biswasb, S. S. Bandyopadhyaya. (2001)"Removal Ofcarbon Dioxide By Absorption In Mixed Amines: Modelling Ofabsorption In Aqueous MDEA/MEA And AMP/MEA Solutions." Chemical Engineering Science 56, 6217–6224,.

Moniuk W., Pohorecki R., (2000). "Absorption Of CO2 In Aqueous Solutions Of N-Methyldiethanolamine ". Inż. Chem. I Proces., 2000, 21, 183-197.

Moomaw, W., F. Yamba, M. Kamimoto, L. Maurice, J. Nyboer, K. Urama, T. Weir, (2011): Introduction. In IPCC Special Report On Renewable Energy

Sources And Climate Change Mitigation, Cambridge University Press, Cambridge, United Kingdom And New York, NY, USA.

Mudhasakul S, Hong-Ming Ku A, Peter L. Douglas(2013). "A Simulation Model Of A CO2 Absorption Process With Methyldiethanolamine Solvent And Piperazine As An Activator." International Journal Of Greenhouse Gas Control 15 , 134–141,.

Onda, K., Sada, E., Saito, M. (1982). "Gas-Side Mass Transfer Coefficients In Packed Towers ". Chem. Eng. Sci. J., 25 (11): 820-829

Pani F., Gaunand A., Cadours R., Bouallou C., Richon D., (1997). "Kinetics Of Absorption Of CO2 In Concentrated Aqueous Methyldiethanolamine Solutions In The Range 296 K To 343 K ". J. Chem. Eng. Data, 1997, 42, 353-359.

Perry R H , Don W. Green,James O. Maloney(1999.). "Perry's Chemical Engineers Handbook." Mcgraw-HILL Companies.

Pinsent B.R.W., Pearson L., Roughton J.W.,(1956). " The Kinetics Of Combination Of Carbon Dioxide With Hydroxideions ". Trans. Faraday Soc., 52, 1512-1516.

Portugal A.F., P.W.J. Derks, G.F. Versteeg, F.D. Magalhães, A. Mendes(2007) "Characterization Of Potassium Glycinate For Carbon Dioxide Absorption Purposes ." Chemical Engineering Science, 2007: 62 , 6534 – 6547.

Reid, R.C., Prausnitz, J.M., Poling, B.E. (1987). " The Properties Of Gases And Liquids 4th Edition "; Mcgraw-Hill Company: New York-USA.

Rinker E.B., Ashour S.S. And Sandall O.C. (1995). " Kinetics And Modeling Of Carbon Dioxide Absorption Into Aqueous Solutions Of N-Methylodiethanolamine ". Chem. Eng. Sci., 50 (5), 755-768

Rochelle*, Manuel A. Pacheco And Gary T(1998). "Rate-Based Modeling Of Reactive Absorption Of CO2 And H2S Into Aqueous Methyldiethanolamine." Ind. Eng. Chem. Res., 37, 4107-4117.

Sandall, Noman Haimour And Orville C(1984). "Absorption Of Carbon Dioxide Into Aqueous Methyldiethanolamin." Chemical Engineermg Science, Vol 39, No. 12. Pp. 1791-1796.

Taylor, R., Krishna, R. (1993). " Multicompo-Nent Mass Transfer "; John Wiley & Sons, Inc.: USA

Vaidya P.D., Kenig E.Y., (2007). "CO2-Alkanolamine Reaction Kinetics: A Review Of Recent Studies ". Chem. Eng. Technol., 30, 1467-1474.

Versteeg.G.F And W. P. M. Van Swaaij (1987)"On The Kinetics Between Co2 And Alkanolamines Both In Aqueous And Non-Aqueous Solutions-Ii. Tertiary Amines." Chemical Engineering Source. Vol. 43. No. 3. Pp. 587-591.

Wang A. Lawal, P. Stephenson, J. Sidders, C. Ramshaw And H. Yeung(2011). "Post-Combustion CO2 Capture With Chemical Absorption: A State-Of-The-Art Review ." Chemical Engineering Research And Design: 89,1609-1624.

Zhao Z, Cui X, Ma J, Li R. (2007), " Adsorption Of Carbon Dioxide On Alkali-Modified Zeolite 13X Adsorbents ". International Journal Of Greenhouse Gas Control, 1:355-359

Zhi Qian, Lianbin Xu, Huibo Cao, And Kai Guo(2009). "Modeling Study On Absorption Of CO2 By Aqueous Solutions Of Nmethyldiethanolamine In Rotating Packed Bed." Ind. Eng. Chem. Res., 48, 9261–9267,.

The Author Biography

Duaa Abdelmonem Amin Ali the author of the thesis was born in Khartoum –Sudan in august 23 1989. And now residing in Surabaya Indonesia .she is the third child of five children. She has formal education including Bitalmal Elementary school and Omdurman high school .She has graduated from university of Khartoum, Faculty of Engineering, Department of Chemical at October 2010 and obtain BSc, From 2010 to 2011 she worked as teacher assistant in the same department and in 2012 She worked for a year as process engineer in gortag factory for solution -Sudan

In 2013 she continue her study to postgraduate level at Institut Teknologi Sepuluh Nopember (ITS),Faculty of Industry Technology ,Chemical Engineering Department .To contact the author the correspondence email Didaaamin@gmail.com